IEEE Access
Multidisciplinary | Rapid Review | Open Access Journal

Received October 12, 2018, accepted October 31, 2018, date of publication November 6, 2018,
date of current version December 18, 2018.

Digital Object Identifier 10.1109/ACCESS.2018.2879901

Performance Optimization for Hybrid Two-Way Cognitive Cooperative Radio Networks With Imperfect Spectrum Sensing

THI MY CHINH CHU, (Member, IEEE),
AND HANS-JÜRGEN ZEPERNICK, (Senior Member, IEEE)
Blekinge Institute of Technology, SE-371 79 Karlskrona, Sweden
Corresponding author: Hans-Jürgen Zepernick (hans-jurgen.zepernick@ieee.org)

ABSTRACT In this paper, we consider a two-way cognitive cooperative radio network (TW-CCRN) with hybrid interweave-underlay spectrum access in the presence of imperfect spectrum sensing. Power allocation strategies are proposed that maximize the sum-rate and minimize the outage probability of the hybrid TW-CCRN. Specifically, based on the state of the primary network (PN), fading conditions, and system parameters, suitable power allocation strategies subject to the interference power constraint of the PN are derived for each transmission scenario of the hybrid TW-CCRN. Given the proposed power allocation strategies, we analyze the sum-rate and outage probability of the hybrid TW-CCRN over Rayleigh fading taking imperfect spectrum sensing into account. Numerical results are presented to illustrate the effect of the arrival rate, interference power threshold, transmit power of the PN, imperfect spectrum sensing, and maximum total transmit power on the sum-rate and outage probability of the hybrid TW-CCRN.

INDEX TERMS Cognitive cooperative radio network, hybrid interweave-underlay spectrum access, two-way communications, power allocation, sum-rate, outage probability.

I. INTRODUCTION

In recent years, radio spectrum has become more and more exhausted due to the increasing demand on bandwidth hungry mobile multimedia services such as mobile gaming, mobile virtual reality, and mobile augmented reality. On the other hand, measurement campaigns conducted by the Federal Communications Commission and other frequency authorities around the world have revealed that the utilisation of the licensed radio spectrum over time and space is rather low [1]–[3]. Advanced radio transmission techniques are therefore required that can more efficiently utilize the scarce and precious radio spectrum. In this context, the cognitive radio (CR) concept has been proposed in [4] to more efficiently utilize radio spectrum. This technique flexibly and intelligently allows secondary users (SUs) to access the spectrum that has been licensed to primary users (PUs) as long as satisfactory quality-of-service (QoS) in the primary network (PN) is maintained.

There exist three main approaches for the SUs to access the radio spectrum licensed to the PUs, i.e., interweave, underlay, and overlay spectrum access [5]. In interweave spectrum access, SUs sense the licensed spectrum and only opportunistically access those spectrum portions that are not occupied by PUs. In this way, interference to the PUs is avoided at the expense of the SUs not being allowed to access the spectrum at any arbitrary time [6]. In contrast, in underlay and overlay spectrum access, SUs can simultaneously access the spectrum with the PUs. Specifically, the SUs in underlay spectrum access continuously adapt their transmit powers to stay below the tolerable interference levels of the PUs [7]. On the other hand, overlay spectrum access relies on cooperation of the SUs with the PUs. As such, sophisticated interference cancelation techniques to alleviate interference to the PUs are needed which incurs challenges on the practical implementation [8].

A. RELATED WORK

Given that the interference from the SUs to the PUs is of major concern, transmit power of the SUs is constrained not only by the maximum power level supported by a particular device technology but also by the maximum interference tolerated by the PUs. As a consequence, SU transmit power has to be kept at rather low levels which in turn causes limitations on system performance. In order to overcome these

difficulties in the secondary network (SN), advanced radio transmission techniques have been developed for conventional cognitive radio networks (CRNs) ranging from adaptive modulation and coding over beamforming transmission to cooperative relaying [9]–[14]. Further, power allocation strategies have been advised, e.g. [15], [16], to reduce interference to the PN and to improve system performance in the CRN.

Aiming to alleviate the performance degradation caused by the transmit power limits imposed on the SUs, cooperative relaying has been incorporated into CRNs which then constitute cognitive cooperative radio networks (CCRNs). A great deal of power allocation algorithms have also been developed recently [17]–[19] that dynamically assign powers among the secondary transmitter and secondary relay aiming at optimizing the performance of CCRNs. In [17], power allocation strategies for an amplify-and-forward (AF) CCRN have been formulated to maximize average network throughput and to minimize approximate outage probability subject to the transmit power limit of the CCRN and the interference power constraint of the PN. In [18], a power allocation strategy to maximize the energy efficiency for a decode-and-forward (DF) CCRN has been proposed. In [20], two optimal power allocation strategies for hybrid interweave-underlay CCRNs in the presence of Rayleigh fading have been developed to maximize channel capacity and to minimize outage probability.

To further improve spectral efficiency, two-way relaying can be deployed to increase the sum-rate of CCRNs [21]–[29]. Specifically, optimal and suboptimal power allocation algorithms have been proposed in [21] to optimize the sum-rate of a beamforming two-way CCRN (TW-CCRN). Further, optimal power allocation along with an AF relay selection scheme using half-duplex communication has been proposed in [22] to maximize the throughput of TW-CCRNs. In [23], a two-way relaying scheme has been proposed that uses best relay selection and a novel cooperative protocol choosing between AF and DF mode to obtain higher sum-rate for the TW-CCRN while keeping interference to the PUs below a given level. Optimal transmit power allocation for multiple-input multiple-output (MIMO) underlay TW-CCRNs employing multiple AF relays has been studied in [24] to maximize the sum-rate of the SU. The work reported in [25] has investigated joint bandwidth and power allocation for MIMO TW-CCRNs and its effect on the achievable cognitive sum-rate. A space alignment technique for a TW-CCRN has been proposed in [26] to protect the SUs from interference from the PUs. On this basis, optimal power allocation has been derived to maximize the secondary achievable sum-rate. Recent work has addressed topics such as max-min optimization of transmit powers in TW-CCRNs [27], power allocation and cooperative diversity in TW-CCRNs [28], and studied TW-CCRNs in which secondary relays assist the transmission of the PUs [29]. However, the works [21]–[29] have focused only on power allocation with underlay spectrum access for TW-CCRNs while interweave, overlay, and hybrid spectrum access have not been considered.

To exploit the advantages and to alleviate the disadvantages of interweave, overlay, and underlay spectrum access, several hybrid spectrum access schemes have been proposed, e.g., [30]–[36]. A hybrid overlay-underlay spectrum access scheme has been proposed in [30] and [31] to exploit not only unused but also under-utilized spectrum regions of the PN. In [32], receive beamforming has been designed subject to an outage-based QoS constraint for primary communication to maximize the achievable average rate of an SU in the uplink of a hybrid interweave-underlay CRN. Furthermore, the performance in terms of throughput for the SU of a hybrid interweave-underlay CRN that incorporates the impact of imperfect channel state information has been analyzed in [33]. In [34], a scheme combining spectrum sensing and recognition of operating power levels at the PUs has been proposed to further improve the detection performance of hybrid interweave-underlay CRNs. In [35] and [36], based on the activity states of the PN, the SUs flexibly utilize interweave and underlay spectrum access, i.e., if a spectrum hole appears, the SUs transmit with maximum power. Once a PU becomes active, the SUs must control their transmit powers to meet the peak interference power constraint of the primary receiver.

In order to implement hybrid spectrum access, spectrum sensing is compulsory and must be performed before each transmission. However, the works [30]–[36] discussed above, assumed that the SUs always perform spectrum sensing accurately such that they can choose interweave or underlay mode correctly. In practice, all spectrum sensing methods are subject to errors caused by various impairments such as interference and noise. In this case, CRNs and CCRNs are not able to perform spectrum sensing perfectly, i.e., false alarm or missed detection may occur with a certain probability. Thus, the effect of imperfect spectrum sensing on the performance of CRNs and CCRNs should be taken into account. Recent research incorporating this aspect of practical deployments include the work reported in [37] which has studied CRNs with directional antennas and imperfect spectrum sensing. Specifically, a lower bound on the ergodic capacity has been derived and the effect of spectrum sensing errors on the bound has been studied. Simulation results have illustrated that directional antennas can alleviate the impact of imperfect spectrum sensing on the bound. In [38], the impact of spectrum sensing errors on the delay and throughput of a cognitive go-back-N hybrid automatic repeat request (HARQ) protocol has been analyzed. Significant performance degradation has been observed when the activity of the PU becomes high or the communication in the CRN becomes less reliable. Similar findings have been reported in [39] with respect to the performance of a cognitive stop-and-wait HARQ protocol in the presence of spectrum sensing errors. In [40], cognitive small cell deployments have been studied accounting for cross-tier interference, imperfect hybrid spectrum sensing, and energy efficiency. An iterative

resource allocation algorithm has been developed to optimize spectrum sensing time and power allocation. Further, power allocation in CRNs in the presence of spectrum sensing errors has been studied aiming at energy-efficiency in sensing-based spectrum sharing CRNs [41], robust power allocation in hybrid overlay-underlay CRNs with orthogonal frequency division multiplexing [42], and robust max-min fairness resource allocation [43].

In light of the directions of resource allocation in CRNs, our work reported in [20] has taken into account the impact of imperfect spectrum sensing on the performance of a hybrid interweave-underlay CCRN. Specifically, two optimal power allocation strategies have been proposed to maximize channel capacity and to minimize outage probability for the SU in the presence of imperfect spectrum sensing. For this purpose, the Karush-Kuhn-Tucker conditions of convex optimization have been used to develop these optimal power allocation strategies. However, in [20], only one-way communications has been considered which does not achieve as high spectrum efficiency as can be offered by two-way communications. In this paper, we therefore advance on previous work by developing optimal power allocation strategies for hybrid interweave-underlay TW-CCRNs with imperfect spectrum access. Applying two-way communications to establish a hybrid TW-CCRN significantly increases functionality and complexity of the system model. In particular, two-way communications allows the SUs to transmit/broadcast their signals at the same time to the secondary relay. Consequently, the secondary relay needs to simultaneously process the signals received from the SUs in the relaying phase and then forwards the resulting signal to the respective SUs. In contrast to [20], due to the more complicated system model of the hybrid TW-CCRN, the optimization problems posed to obtain optimal power allocation cannot be formulated in convex forms. Specifically, optimal power allocation strategies are derived by converting the posed non-convex geometric programming standard form problems into convex optimization problems along with adapting the standard barrier-based interior-point method. To the best of our knowledge, there has been no work focusing on deploying hybrid interweave-underlay spectrum access with TW-CCRNs along with investigating the influence of imperfect spectrum sensing on the performance of such hybrid TW-CCRNs.

B. CONTRIBUTIONS AND PAPER STRUCTURE

In view of the above discussion, in this paper, we develop optimal power allocation strategies for TW-CCRNs using hybrid interweave-underlay spectrum access to enhance spectrum utilization while accounting for spectrum sensing errors. Specifically, by considering both the total transmit power limit of the hybrid TW-CCRN and the interference power constraint of the PN, we propose power allocation strategies that maximize sum-rate and minimize outage probability of the hybrid TW-CCRN. Numerical results are provided to examine the effect of imperfect spectrum sensing such as false alarm and missed detection on sum-rate and outage probability of the system. Further, the effect of the traffic characteristics of both the PU and SUs, the transmit power limit of the SUs, and the interference power constraint of the PN on the performance of the hybrid TW-CCRN is studied. Finally, comparisons of the performance of the hybrid TW-CCRN with optimal power allocation and equal power allocation are provided to illustrate the performance improvement of the proposed power allocation strategies. In summary, major contributions of this paper can be stated as follows:

- Two-way communications, hybrid interweave-underlay spectrum access, and AF relaying are combined to establish a hybrid TW-CCRN in order to support improved system performance over Rayleigh fading.
- Optimal power allocation strategies are proposed to maximize sum-rate and to minimize outage probability of the hybrid TW-CCRN.
- Optimization algorithms are developed that solve the optimal power allocation problems based on converting the non-convex geometric programming standard form problems into convex optimization problems by adapting the standard barrier-based interior-point method.
- Performance is assessed in terms of sum-rate and outage probability taking into account the practical issue of imperfect spectrum sensing.
- The impact of fading, traffic statistics of both the PN and hybrid TW-CCRN, the interference power constraint imposed by the PN, and the maximum transmit power limit of the hybrid TW-CCRN are included into the performance analysis.
- Performance comparisons of the sum-rate and outage probability of the hybrid TW-CCRN with and without the proposed power allocation strategies are provided.

The rest of this paper is organized as follows. Section II describes the system model and derives expressions for the instantaneous signal-to-noise ratio (SNR) and signal-plus-interference-to-noise ratio (SINR) of the hybrid TW-CCRN for each operation scenario. Section III and IV propose optimal power allocation strategies that maximize sum-rate and minimize outage probability of the hybrid TW-CCRN, respectively. Numerical results for the sum-rate and outage probability of the hybrid TW-CCRN are provided in Section V. Finally, a summary of the paper is given in Section VI.

II. SYSTEM MODEL

We consider a hybrid TW-CCRN that operates in the presence of a PN as shown in Fig. 1. The hybrid TW-CCRN consists of two SUs where SU_1 communicates with SU_2 through the support of an AF secondary relay SU_R and vice versa. Further, the PN consists of a primary transmitter PU_{TX} and a primary receiver PU_{RX}. It is assumed that both, the hybrid TW-CCRN and the PN, are subject to block Rayleigh fading. The channel coefficients of the two-way communication links $SU_1 \leftrightarrows SU_R$, $SU_2 \leftrightarrows SU_R$, and interference links $SU_1 \rightarrow PU_{RX}$, $SU_R \rightarrow PU_{RX}$, $SU_2 \rightarrow PU_{RX}$, $PU_{TX} \rightarrow SU_1$,

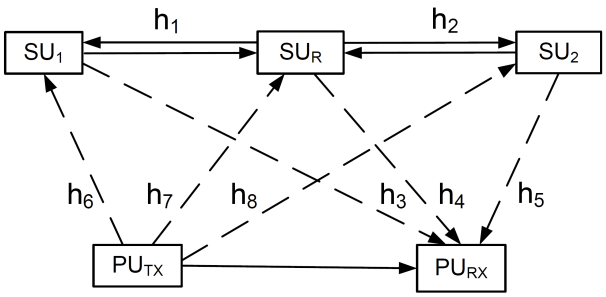

FIGURE 1. Topology of the considered hybrid interweave-underlay TW-CCRN (Solid lines: Communication links; Dashed lines: Interference links).

$PU_{TX} \rightarrow SU_R$, and $PU_{TX} \rightarrow SU_2$ are, respectively, denoted as h_1, h_2, h_3, h_4, h_5, h_6, h_7, and h_8. The communication of the hybrid TW-CCRN is organised into two time slots (TSs). In the first TS, both SU_1 and SU_2 broadcast their transmit signals to SU_R. In the second TS, SU_R amplifies the received signals and then forwards the resulting signals to SU_1 and SU_2. A potential deployment scenario for this system model could be small cell cognitive radio networks in the context of 5G mobile networks.

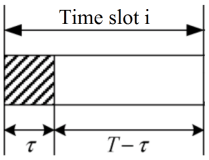

FIGURE 2. Time slot structure for sensing-based spectrum sharing (τ: sensing duration; $T - \tau$: data transmission duration).

In this TW-CCRN, we deploy hybrid interweave-underlay spectrum access at all secondary users, i.e., SU_1, SU_2, and SU_R. Depending on the sensed state of the PN being active or inactive, each SU selects the suitable spectrum access mode in each of the two TSs. For this purpose, each TS is further structured into a sensing phase which is followed by a transmission phase [44] as in Fig. 2. In the first phase, the SUs independently sense the licensed spectrum to reveal the state of the PU_{TX}. Due to SU_1, SU_2, and SU_R typically being at different locations, their sensing outcomes after the same sensing duration τ may also be different. To enhance the accuracy of spectrum sensing, we employ cooperative sequential spectrum sensing where SUs mutually exchange their sensing results [45]. In this way, the accuracy of the overall sensing results can be enhanced significantly and all SUs have the same false alarm and missed detection probability after the sensing phase. After exchanging the sensing results, if PU_{TX} is sensed to be inactive, the SUs are not subject to an interference constraint and can utilize the interweave mode in the transmission phase. If PU_{TX} is sensed to be active, the SUs must operate in underlay mode during the transmission phase and control their transmit powers to not exceed the interference threshold Q imposed by the PU_{RX}. Due to the sensing phase, the SUs do not commence with data transmission at the beginning of each TS but with a delay that is equivalent to the sensing duration. Because the sensing duration is typically small in the order of 1 ms compared to the data transmission duration of, e.g., 100 ms, the SUs are assumed to start transmission at the beginning of each TS [46]. Accordingly, the SUs remain in the selected spectrum access mode for the during of a TS and adapt their access mode in the subsequent TS if needed. Depending on the sensing outcome in each of the two TSs, the transmission of the hybrid TW-CCRN can be classified into the following four scenarios:

- **Scenario 1:** The PN is sensed to be active in both TSs. In this case, the hybrid TW-CCRN uses underlay spectrum access in both TSs and allocates the transmit powers P_{11}, P_{21}, and P_{r1} to SU_1, SU_2, and SU_R, respectively.
- **Scenario 2:** The PN is sensed to be active only in the first TS. Accordingly, underlay spectrum access is used in the first TS and interweave spectrum access is used in the second TS. In this case, the transmit powers P_{12}, P_{22}, and P_{r2}, are allocated to SU_1, SU_2, and SU_R, respectively.
- **Scenario 3:** The PN is sensed to be active only in the second TS. As such, the system uses interweave spectrum access in the first TS and underlay spectrum access in the second TS. In this scenario, the transmit powers P_{13}, P_{23}, and P_{r3} are used at SU_1, SU_2, and SU_R, respectively.
- **Scenario 4:** The PN is sensed to be inactive in both TSs. Then, interweave spectrum access is used in both TSs with transmit powers P_{14}, P_{24}, and P_{r4}, respectively, being allocated to SU_1, SU_2, and SU_R.

Let x_1 and x_2 denote the transmit signals with unit power of SU_1 and SU_2, respectively. Then, the received signal at SU_R in the first TS of Scenario i, $i = 1, 2, 3, 4$, is given by

$$y_{ri}^{(j)} = \sqrt{P_{1i}}h_1x_1 + \sqrt{P_{2i}}h_2x_2 + n_r^{(j)} \tag{1}$$

where $j \in \{0, 1\}$ stands for the actual state of the PN in the first TS, i.e., $j=0$ if the PN is inactive and $j=1$ if it is active.

Further, $n_r^{(j)}$ denotes the noise (or the interference plus noise) at SU_R when the PN is in State j in the first TS. Specifically, if the PN is inactive in the first TS, $n_r^{(0)}$ is the additive white Gaussian noise (AWGN) at SU_R with zero-mean and variance $N_r^{(0)} = N_0$. If the PN is active in the first TS, $n_r^{(1)}$ denotes the interference from the PN to SU_R plus AWGN at SU_R. As suggested in [47] and [48], we can approximate $n_r^{(1)}$ as AWGN with zero-mean and variance

$$N_r^{(1)} = N_0 + P_p d_7^{-n} \tag{2}$$

The second term in (2) is the interference power from PU_{TX} to SU_R following the exponentially decaying path loss model. Here, P_p is the transmit power of PU_{TX}, d_7 is the distance from PU_{TX} to SU_R, and n is the path loss exponent. In summary, the noise term $n_r^{(j)}$ if PN is active or inactive can be modeled as AWGN with zero-mean and variance

$$N_r^{(j)} = N_0 + jP_p d_7^{-n}, \quad j = 0, 1 \tag{3}$$

In the second TS, given Scenario i and State j of the PN, the SU_R amplifies the received signal $y_{ri}^{(j)}$ with gain

$$G_i^{(j)} = \sqrt{\frac{P_{ri}}{P_{1i}|h_1|^2 + P_{2i}|h_2|^2 + N_r^{(j)}}} \tag{4}$$

and subsequently forwards the resulting signal. Then, the received signals at SU_1 and SU_2 in the second TS for Scenario i are, respectively, expressed as

$$y_{1i}^{(jk)} = G_i^{(j)}\sqrt{P_{1i}}h_1^2 x_1 + G_i^{(j)}\sqrt{P_{2i}}h_1 h_2 x_2 + G_i^{(j)} h_1 n_r^{(j)} + n_1^{(k)} \tag{5}$$

$$y_{2i}^{(jk)} = G_i^{(j)}\sqrt{P_{1i}}h_1 h_2 x_1 + G_i^{(j)}\sqrt{P_{2i}}h_2^2 x_2 + G_i^{(j)} h_2 n_r^{(j)} + n_2^{(k)} \tag{6}$$

where $k \in \{0, 1\}$ represents the actual state of the PN in the second TS, i.e., $k = 0$ if the PN is inactive and $k = 1$ if it is active. Similar as in the first TS for SU_R, the noises $n_1^{(k)}$ and $n_2^{(k)}$ at SU_1 and SU_2 subject to the PN being in State k, respectively, are modeled as AWGNs with zero-mean and variances

$$N_1^{(k)} = N_0 + kP_p d_6^{-n}, \quad k = 0, 1 \tag{7}$$

$$N_2^{(k)} = N_0 + kP_p d_8^{-n}, \quad k = 0, 1 \tag{8}$$

where d_6 is the distance from PU_{TX} to SU_1 and d_8 is the distance from PU_{TX} to SU_2. Since SU_1 knows its transmit signal x_1 and is assumed to have perfect channel state information (CSI) in terms of channel coefficient h_1 from SU_1 to SU_R while SU_2 knows its transmit signal x_2 and has perfect CSI in terms of channel coefficient h_2 from SU_2 to SU_R, both SU_1 and SU_2 can subtract the respective superimposed signals $G_i^{(j)}\sqrt{P_{1i}}h_1^2\, x_1$ and $G_i^{(j)}\sqrt{P_{2i}}h_2^2\, x_2$ from their received signals. Regarding efficient approaches for estimating CSI and feeding it back to the respective terminals, we refer to the work reported in [49]–[51]. Therefore, the SNR (PN is inactive) or SINR (PN is active) $\gamma_{1i}^{(jk)}$ at SU_1 and $\gamma_{2i}^{(jk)}$ at SU_2 in Scenario i can be, respectively, obtained as

$$\gamma_{1i}^{(jk)} = \frac{P_{2i}P_{ri}X_1X_2}{P_{ri}X_1N_r^{(j)} + P_{1i}X_1N_1^{(k)} + P_{2i}X_2N_1^{(k)} + N_r^{(j)}N_1^{(k)}} \tag{9}$$

$$\gamma_{2i}^{(jk)} = \frac{P_{1i}P_{ri}X_1X_2}{P_{ri}X_2N_r^{(j)} + P_{1i}X_1N_2^{(k)} + P_{2i}X_2N_2^{(k)} + N_r^{(j)}N_2^{(k)}} \tag{10}$$

with channel power gains $X_1 = |h_1|^2$ and $X_2 = |h_2|^2$. Further, the interference power Q_{1i} from SU_1 and SU_2 to PU_{RX} in the first TS and Q_{2i} from SU_R to PU_{RX} in the second TS of Scenario i are formulated as

$$Q_{1i} = P_{1i}X_3 + P_{2i}X_5 \tag{11}$$

$$Q_{2i} = P_{ri}X_4 \tag{12}$$

where $X_3 = |h_3|^2$, $X_4 = |h_4|^2$, and $X_5 = |h_5|^2$ are the respective channel power gains. Considering Rayleigh fading with channel mean power $\Omega_l = \mathbb{E}\{X_l\}$, the probability density function (PDF) and cumulative distribution function (CDF) of the channel power gain X_l, $l \in \{1, 2, 3, 4, 5\}$, are given by

$$f_{X_l}(x_l) = \frac{1}{\Omega_l}\exp\left(-\frac{x_l}{\Omega_l}\right) \tag{13}$$

$$F_{X_l}(x_l) = 1 - \exp\left(-\frac{x_l}{\Omega_l}\right) \tag{14}$$

In (13) and (14), the channel mean powers Ω_l, $l = 1, \ldots, 8$, are attenuated with distance following the exponentially decaying path loss model with path loss exponent n, i.e., $\mathbb{E}\{X_l\} = \Omega_l \sim d_l^{-n}$.

III. SUM-RATE OPTIMIZATION

In view of [36] and [52], the sum-rate of the considered hybrid TW-CCRN can be formulated as

$$R = \sum_{i=1}^{4}\sum_{j=0}^{1}\sum_{k=0}^{1} p_i^{(jk)}\left(R_{1i}^{(jk)} + R_{2i}^{(jk)}\right) \tag{15}$$

where $p_i^{(jk)}$ denotes the probability that the hybrid TW-CCRN operates in Scenario i when the PN is in State j in the first TS and in State k in the second TS. Note that the probabilities $p_i^{(jk)}$ for each scenario and each PN state are derived in Appendix A taking the traffic statistics of the SUs and PU as well as imperfect spectrum sensing at the SUs into account. Furthermore, $R_{1i}^{(jk)}$ and $R_{2i}^{(jk)}$ are the rates on the links $SU_2 \rightarrow SU_1$ and $SU_1 \rightarrow SU_2$ for Scenario i while the PN is in State j in the first TS and in State k in the second TS. In view of the Shannon capacity theorem, $R_{1i}^{(jk)}$ and $R_{2i}^{(jk)}$ can be calculated as

$$R_{ti}^{(jk)} = \frac{1}{2}\log(1 + \gamma_{ti}^{(jk)}), \quad t = 1, 2 \tag{16}$$

where $\gamma_{1i}^{(jk)}$ and $\gamma_{2i}^{(jk)}$ are, respectively, the instantaneous SNRs/SINRs at SU_1 and SU_2 of Scenario i while the PN is in State j in the first TS and in State k in the second TS.

Let us now commence with deriving a power allocation strategy for the SUs that maximizes the sum-rate of the hybrid TW-CCRN. Given the total transmit power limit P_{T1} in the first TS and P_{T2} in the second TS, the transmit powers of SU_1, SU_2, and SU_R must satisfy the constraints

$$P_{1i} + P_{2i} \le P_{T1} \quad \text{and} \quad P_{ri} \le P_{T2} \tag{17}$$

In addition, when PU is active, the SUs must control their transmit powers to not exceed the interference power threshold Q imposed by PU_{RX}. Thus, the following interference power constraints must be considered in the first and second TS:

$$P_{1i}X_3 + P_{2i}X_5 \le Q \tag{18}$$

$$P_{ri}X_4 \le Q \tag{19}$$

SU_1 and SU_2 consider (18) in Scenarios 1 and 2 when the PU is sensed as active in the first TS while SU_R considers (19) in Scenarios 1 and 3 when the PU is sensed as active in

the second TS. Thus, the problem of maximizing the sum-rate of the hybrid TW-CCRN in Scenario i can be posed as

$$\max_{P_{1i},P_{2i},P_{ri}} \frac{1}{2}\mathbb{E}\{\log[(1+\gamma_{1i}^{(jk)})(1+\gamma_{2i}^{(jk)})]\} \tag{20}$$

$$s.t. \begin{cases} P_{1i}, P_{2i}, P_{ri} & > 0 \\ P_{T1} - (P_{1i} + P_{2i} + 0P_{ri}) & \geq 0 \\ P_{T2} - (0P_{1i} + 0P_{2i} + P_{ri}) & \geq 0 \\ Q - 1_{[i=1 \text{ or } 2]}(X_3P_{1i} + X_5P_{2i} + 0P_{ri}) & \geq 0 \\ Q - 1_{[i=1 \text{ or } 3]}(0P_{1i} + 0P_{2i} + X_4P_{ri}) & \geq 0 \end{cases} \tag{21}$$

where $1_{[\cdot]}$ is the indication function which returns 1 if the condition in $[\cdot]$ is correct. Otherwise, the function returns 0.

Applying the decomposition method of [53], the objective (20) subject to (21) can be decoupled into parallel sub-objectives each being subject to (21), i.e.,

$$\max_{P_{1i},P_{2i},P_{ri}} \log[(1+\gamma_{1i}^{(jk)})(1+\gamma_{2i}^{(jk)})] \tag{22}$$

In other words, sub-objective (22) maximizes the sum-rate of the hybrid TW-CCRN for each transmission from SU_1 to SU_2 and from SU_2 to SU_1. As the logarithm is an increasing function, finding the maximum sum-rate of (22) subject to (21) is equivalent to finding the maximum of $(1+\gamma_{1i}^{(jk)})(1+\gamma_{2i}^{(jk)})$. This problem is equivalent to finding the minimum of $1/(\gamma_{1i}^{(jk)}\gamma_{2i}^{(jk)})$ subject to (21). Then, a solution of (22) subject to (21) can be obtained by solving the problem

$$\min_{P_{1i},P_{2i},P_{ri}} f_i^{(jk)}(P_{1i}, P_{2i}, P_{ri}) \tag{23}$$

The objective function $f_i^{(jk)}(P_{1i}, P_{2i}, P_{ri}) = 1/(\gamma_{1i}^{(jk)}\gamma_{2i}^{(jk)})$ in (23) is obtained with (9) and (10) as

$$\begin{aligned} f_i^{(jk)}&(P_{1i}, P_{2i}, P_{ri}) \\ &= c_1P_{1i}^{-1}P_{2i}^{-1} + c_2P_{1i}^{-1}P_{ri}^{-1} + c_3P_{2i}^{-1}P_{ri}^{-1} \\ &\quad + c_4P_{1i}P_{2i}^{-1}P_{ri}^{-2} + c_5P_{1i}^{-1}P_{2i}P_{ri}^{-2} + c_6P_{ri}^{-2} + c_7P_{1i}^{-1}P_{ri}^{-2} \\ &\quad + c_8P_{2i}^{-1}P_{ri}^{-2} + c_9P_{1i}^{-1}P_{2i}^{-1}P_{ri}^{-1} + c_{10}P_{1i}^{-1}P_{2i}^{-1}P_{ri}^{-2} \end{aligned} \tag{24}$$

where

$$\begin{aligned} c_1 &= \frac{(N_r^{(j)})^2}{X_1X_2} \\ c_2 &= \frac{N_2^{(k)}N_r^{(j)}X_1 + N_1^{(k)}N_r^{(j)}X_2}{X_1^2X_2} \\ c_3 &= \frac{N_2^{(k)}N_r^{(j)}X_1 + N_1^{(k)}N_r^{(j)}X_2}{X_1X_2^2} \\ c_4 &= N_1^{(k)}N_2^{(k)}/X_2^2 \\ c_5 &= N_1^{(k)}N_2^{(k)}/X_1^2 \\ c_6 &= \frac{2N_1^{(k)}N_2^{(k)}}{X_1X_2} \\ c_7 &= \frac{2N_1^{(k)}N_2^{(k)}N_r^{(j)}}{X_1^2X_2} \\ c_8 &= \frac{2N_1^{(k)}N_2^{(k)}N_r^{(j)}}{X_1X_2^2} \\ c_9 &= \frac{(N_1^{(k)})^2X_2 + (N_2^{(k)})^2X_1}{X_1^2X_2^2} \\ c_{10} &= \frac{N_1^{(k)}N_2^{(k)}(N_r^{(j)})^2}{X_1^2X_2^2} \end{aligned} \tag{25}$$

Because the objective and inequality constraint functions are posynomials, problem (23) subject to (21) is in geometric programming (GP) standard form. Since a posynomial is not convex, the optimization problem in GP standard form is not convex. Thus, we need to transform (23) into a convex optimization problem. Since $\exp(\log(x)) = x$, we first change problem (23) into the following convex optimization problem:

$$\min_{p_{1i},p_{2i},p_{ri}} g_i^{(jk)}(p_{1i}, p_{2i}, p_{ri}) \tag{26}$$

$$s.t. \begin{cases} p_{1i}, p_{2i}, p_{ri} & > 0 \\ \exp(p_{1i} + b_{11}) + \exp(p_{2i} + b_{12}) & \leq 1 \\ \exp(p_{ri} + b_{21}) & \leq 1 \\ 1_{[i=1 \text{ or } 2]}\left[\exp(p_{1i} + b_{31}) + \exp(p_{2i} + b_{32})\right] & \leq 1 \\ 1_{[i=1 \text{ or } 3]}\left[\exp(p_{ri} + b_{41})\right] & \leq 1 \end{cases} \tag{27}$$

where objective function $g_i^{(jk)}(p_{1i}, p_{2i}, p_{ri})$ is given as

$$\begin{aligned} &g_i^{(jk)}(p_{1i}, p_{2i}, p_{ri}) \\ &= \exp(-p_{1i} - p_{2i} + b_{01}) + \exp(-p_{1i} - p_{ri} \\ &\quad + b_{02}) + \exp(-p_{2i} - p_{ri} + b_{03}) + \exp(p_{1i} - p_{2i} - 2p_{ri} + b_{04}) \\ &\quad + \exp(-p_{1i} + p_{2i} - 2p_{ri} + b_{05}) + \exp(-2p_{ri} + b_{06}) + \exp(-p_{1i} \\ &\quad - 2p_{ri} + b_{07}) + \exp(-p_{2i} - 2p_{ri} + b_{08}) + \exp(-p_{1i} - p_{2i} \\ &\quad - p_{ri} + b_{09}) + \exp(-p_{1i} - p_{2i} - 2p_{ri} + b_{010}) \end{aligned} \tag{28}$$

The following abbreviations have been introduced in (28):

$$p_{1i} = \log P_{1i},\ p_{2i} = \log P_{2i},\ p_{ri} = \log P_{ri}, \quad i = 1, 2, 3, 4 \tag{29}$$

$$\begin{aligned} b_{0a} &= \log c_a, \quad a = 1, \ldots, 10 \\ b_{11} &= \log \frac{1}{P_{T1}} \quad b_{21} = \log \frac{1}{P_{T2}} \quad b_{32} = \log \frac{X_5}{Q} \\ b_{12} &= \log \frac{1}{P_{T1}} \quad b_{31} = \log \frac{X_3}{Q} \quad b_{41} = \log \frac{X_4}{Q} \end{aligned} \tag{30}$$

Then, using the logarithmic transform, problem (23) can be converted into the following convex optimization problem:

$$\min_{\mathbf{p}_i} \log \sum_{a=1}^{A_0} \exp\left(\mathbf{a}_{0a}^T\mathbf{p}_i + b_{0a}\right) \tag{31}$$

$$s.t.\begin{cases}\mathbf{p}_i & \succ 0\\ \log\sum_{a=1}^{A_1}\exp(\mathbf{a}_{1a}^T\mathbf{p}_i+b_{1a}) & \le 0\\ \log\sum_{a=1}^{A_2}\exp(\mathbf{a}_{2a}^T\mathbf{p}_i+b_{2a}) & \le 0\\ 1_{[i=1\text{ or }2]}\log\sum_{a=1}^{A_3}\exp(\mathbf{a}_{3a}^T\mathbf{p}_i+b_{3a}) & \le 0\\ 1_{[i=1\text{ or }3]}\log\sum_{a=1}^{A_4}\exp(\mathbf{a}_{4a}^T\mathbf{p}_i+b_{4a}) & \le 0\end{cases} \tag{32}$$

where $\mathbf{p}_i=[p_{1i}\ p_{1i}\ p_{ri}]^T$, $A_0=10$, $A_1=A_3=2$, $A_2=A_4=1$, and

$$\begin{aligned}
\mathbf{a}_{01}&=[-1\ -1\ 0]^T\\
\mathbf{a}_{02}&=[-1\ 0\ -1]^T\\
\mathbf{a}_{03}&=[0\ -1\ -1]^T\\
\mathbf{a}_{04}&=[1\ -1\ -2]^T\\
\mathbf{a}_{05}&=[-1\ 1\ -2]^T\\
\mathbf{a}_{06}&=[0\ 0\ -2]^T\\
\mathbf{a}_{07}&=[-1\ 0\ -2]^T\\
\mathbf{a}_{08}&=[0\ -1\ -2]^T\\
\mathbf{a}_{09}&=[-1\ -1\ -1]^T\\
\mathbf{a}_{10}&=[-1\ -1\ -2]^T\\
\mathbf{a}_{11}&=[1\ 0\ 0]^T\\
\mathbf{a}_{12}&=[0\ 1\ 0]^T\\
\mathbf{a}_{21}&=[0\ 0\ 1]^T\\
\mathbf{a}_{31}&=[1\ 0\ 0]^T\\
\mathbf{a}_{32}&=[0\ 1\ 0]^T\\
\mathbf{a}_{41}&=[0\ 0\ 1]^T
\end{aligned} \tag{33}$$

As in [54]–[56], the log-sum-exp function of a variable $\mathbf{x}=[x_1,\ldots,x_n]^T$, i.e., $f(\mathbf{x})=\log\sum_{i=1}^n\exp(x_i)$ leads to a convex problem in $\mathbf{x}$. Thus, problem (31) subject to (32) is convex which can be solved by using the standard barrier-based interior-point method [53], [57]. The idea of this method is to solve a sequence of unconstrained problems that absorb the constraints into a new objective function which is a weighted sum of the original objective function and the log-barrier function of the constraints. To utilize the standard barrier-based interior-point method, we must convert the above inequality constraint optimization problem into an unconstrained optimization problem. Specifically, applying the logarithmic barrier function, problem (31) subject to (32) can be approximated as unconstrained optimization problem

$$\min_{\mathbf{p}_i}\left\{w\,h_i^{(jk)}(\mathbf{p}_i)+\phi_i^{(jk)}(\mathbf{p}_i)\right\} \tag{34}$$

where w is the chosen weight of the original objective function

$$h_i^{(jk)}(\mathbf{p}_i)=\log\sum_{a=1}^{A_0}\exp(\mathbf{a}_{0a}^T\,\mathbf{p}_i+b_{0a}) \tag{35}$$

As w becomes larger, the unconstrained problem becomes a tighter approximation of the original problem. Further, $\phi_i^{(jk)}(\mathbf{p}_i)$ in (34) is defined as

$$\phi_i^{(jk)}(\mathbf{p}_i)=\begin{cases}-\sum_{l=1}^{4}\log\left[-\log\sum_{a=1}^{A_l}\exp\left(\mathbf{a}_{la}^T\mathbf{p}_i+b_{la}\right)\right], & i=1\\ -\sum_{l=1}^{3}\log\left[-\log\sum_{a=1}^{A_l}\exp\left(\mathbf{a}_{la}^T\mathbf{p}_i+b_{la}\right)\right], & i=2\\ -\sum_{l=1}^{2}\log\left[-\log\sum_{a=1}^{A_l}\exp\left(\mathbf{a}_{la}^T\mathbf{p}_i+b_{la}\right)\right] & \\ -\log\left[-\log(\exp(\mathbf{a}_{4a}^T\mathbf{p}_i+b_{4a}))\right], & i=3\\ -\sum_{l=1}^{2}\log\left[-\log\sum_{a=1}^{A_l}\exp\left(\mathbf{a}_{la}^T\mathbf{p}_i+b_{la}\right)\right], & i=4\end{cases} \tag{36}$$

A procedure based on the barrier-method algorithm to find a solution to optimization problem (34) is given in Appendix B.

IV. OUTAGE PROBABILITY OPTIMIZATION FOR THE SECONDARY NETWORK

Applying [20] and [52], the outage probability $P_o^{\mathrm{SU}_1}$ of SU_1 and $P_o^{\mathrm{SU}_2}$ of SU_2, respectively, can be expressed as

$$P_o^{\mathrm{SU}_1}=\sum_{i=1}^{4}\sum_{j=0}^{1}\sum_{k=0}^{1}p_i^{(jk)}F_{\gamma_{1i}^{(jk)}}(\gamma_{th1}) \tag{37}$$

$$P_o^{\mathrm{SU}_2}=\sum_{i=1}^{4}\sum_{j=0}^{1}\sum_{k=0}^{1}p_i^{(jk)}F_{\gamma_{2i}^{(jk)}}(\gamma_{th2}) \tag{38}$$

where $F_{\gamma_{1i}^{(jk)}}(\gamma)$ and $F_{\gamma_{2i}^{(jk)}}(\gamma)$ are, respectively, the CDFs of the instantaneous SINRs/SNRs $\gamma_{1i}^{(jk)}$ at SU_1 and $\gamma_{2i}^{(jk)}$ at SU_2 in Scenario i. From (9), $F_{\gamma_{1i}^{(jk)}}(\gamma)$ can be expressed as

$$\begin{aligned}
&F_{\gamma_{1i}^{(jk)}}(\gamma)\\
&=F_{X_2}\left(\frac{(P_{1i}N_1^{(k)}+P_{ri}N_r^{(j)})\gamma}{P_{2i}P_{ri}}\right)+\frac{1}{P_{2i}P_{ri}}\\
&\quad\times\int_0^{\infty}F_{X_1}\left(\frac{\gamma N_1^{(k)}(x+(P_{1i}N_1^{(k)}+P_{ri}N_r^{(j)})\gamma+P_{ri}N_r^{(j)})}{P_{ri}x}\right)\\
&\quad\times f_{X_2}\left(\frac{x+\left(P_{1i}N_1^{(k)}+P_{ri}N_r^{(j)}\right)\gamma}{P_{2i}P_{ri}}\right)dx
\end{aligned} \tag{39}$$

Substituting (13) and (14) into (39) along with the help of [58, eq. (3.471.9)], we obtain

$$\begin{aligned} F_{\gamma_{1i}^{(jk)}}(\gamma) &= 1 - \frac{\exp\left(-\frac{(P_{1i}N_1^{(k)}+P_{ri}N_r^{(j)})\Omega_1\gamma+P_{2i}N_1^{(k)}\Omega_2\gamma}{P_{2i}P_{ri}\Omega_1\Omega_2}\right)}{P_{2i}P_{ri}\Omega_2} \\ &\quad \times 2\sqrt{\frac{P_{1i}P_{2i}(N_1^{(k)})^2\Omega_2\gamma^2 + P_{2i}P_{ri}N_1^{(k)}N_r^{(j)}\Omega_2(\gamma+1)\gamma}{\Omega_1}} \\ &\quad \times \mathcal{K}_1\left(2\sqrt{\frac{P_{1i}(N_1^{(k)})^2\gamma^2 + P_rN_1^{(k)}N_r^{(j)}(\gamma+1)\gamma}{P_{2i}P_{ri}^2\Omega_1\Omega_2}}\right) \end{aligned} \tag{40}$$

where $\mathcal{K}_1(\cdot)$ stands for the first order modified Bessel function of the second kind [58, eq. (8.432.1)].

For high SINR/SNR, we use the approximations $\mathcal{K}_1(2x) \approx 1/x$ and $\exp(-x) \approx 1-x$ as in [59]. Then, (40) and similarly the CDF of $\gamma_{2i}^{(jk)}$ at SU_2 in Scenario i are obtained as

$$F_{\gamma_{1i}^{(jk)}}(\gamma) = \frac{P_{1i}N_1^{(k)}\gamma}{P_{2i}P_{ri}\Omega_2} + \frac{N_r^{(j)}\gamma}{P_{2i}\Omega_2} + \frac{N_1^{(k)}\gamma}{P_{ri}\Omega_1} \tag{41}$$

$$F_{\gamma_{2i}^{(jk)}}(\gamma) = \frac{P_{2i}N_2^{(k)}\gamma}{P_{1i}P_{ri}\Omega_1} + \frac{N_r^{(j)}\gamma}{P_{1i}\Omega_1} + \frac{N_2^{(k)}\gamma}{P_{ri}\Omega_2} \tag{42}$$

Let as now focus on minimizing the outage probability of the hybrid TW-CCRN which falls into outage if any transmission from SU_1 to SU_2 or vice versa falls into outage. We are aiming at a power allocation strategy that minimizes the maximum outage probability at SU_1 and SU_2. Given Scenario i, this optimization problem subject to (21) can be posed as

$$\min_{P_{1i}P_{2i},P_{ri}} \max\left\{F_{\gamma_{1i}^{(jk)}}(\gamma_{th1}), F_{\gamma_{2i}^{(jk)}}(\gamma_{th2})\right\} \tag{43}$$

By introducing the auxiliary variable

$$V_i = \max\left\{F_{\gamma_{1i}^{(jk)}}(\gamma_{th1}), F_{\gamma_{2i}^{(jk)}}(\gamma_{th2})\right\} \tag{44}$$

we can rewrite (43) as (see also Appendix C)

$$\min_{P_{1i}P_{2i},P_{ri},V_i} V_i \tag{45}$$

$$s.t. \begin{cases} P_{1i},\ P_{2i},\ P_{ri},\ V_i & > 0 \\ P_{1i}+P_{2i} & \le P_{T1} \\ P_{ri} & \le P_{T2} \\ 1_{[i=1 \text{ or } 2]}(P_{1i}X_3 + P_{2i}X_5) & \le Q \\ 1_{[i=1 \text{ or } 3]}P_{ri}X_4 & \le Q \\ \frac{P_{1i}N_1^{(k)}\gamma}{P_{2i}P_{ri}\Omega_2} + \frac{N_r^{(j)}\gamma}{P_{2i}\Omega_2} + \frac{N_1^{(k)}\gamma}{P_{ri}\Omega_1} & \le V_i \\ \frac{P_{2i}N_2^{(k)}\gamma}{P_{1i}P_{ri}\Omega_1} + \frac{N_r^{(j)}\gamma}{P_{1i}\Omega_1} + \frac{N_2^{(k)}\gamma}{P_{ri}\Omega_2} & \le V_i \end{cases} \tag{46}$$

Again, as the objective and all inequality constraint functions are posynomials, problem (45) subject to (46) is in GP standard form and is not convex. Similar as for the sum-rate, we transform this GP into a convex optimization problem as

$$\min_{\bar{\mathbf{p}}_i} \log \sum_{a=1}^{\bar{A}_0} \exp(\bar{\mathbf{a}}_{0a}^T\bar{\mathbf{p}}_i + \bar{b}_{0a}) \tag{47}$$

$$s.t. \begin{cases} \bar{\mathbf{p}}_i & \succ 0 \\ \log \sum_{a=1}^{\bar{A}_1} \exp(\bar{\mathbf{a}}_{1a}^T\bar{\mathbf{p}}_i + \bar{b}_{1a}) & \le 0 \\ \log \sum_{a=1}^{\bar{A}_2} \exp(\bar{\mathbf{a}}_{2a}^T\bar{\mathbf{p}}_i + \bar{b}_{2a}) & \le 0 \\ 1_{[i=1 \text{ or } 2]} \log \sum_{a=1}^{\bar{A}_3} \exp(\bar{\mathbf{a}}_{3a}^T\bar{\mathbf{p}}_i + \bar{b}_{3a}) & \le 0 \\ 1_{[i=1 \text{ or } 3]} \log \sum_{a=1}^{\bar{A}_4} \exp(\bar{\mathbf{a}}_{4a}^T\bar{\mathbf{p}}_i + \bar{b}_{4a}) & \le 0 \\ \log \sum_{a=1}^{\bar{A}_5} \exp(\bar{\mathbf{a}}_{5a}^T\bar{\mathbf{p}}_i + \bar{b}_{5a}) & \le 0 \\ \log \sum_{a=1}^{\bar{A}_6} \exp(\bar{\mathbf{a}}_{6a}^T\bar{\mathbf{p}}_i + \bar{b}_{6a}) & \le 0 \end{cases} \tag{48}$$

where $\bar{\mathbf{p}}_i = [p_{1i}\ p_{2i}\ p_{ri}\ v_i]^T$ with $p_{1i} = \log P_{1i}$, $p_{2i} = \log P_{2i}$, $p_{ri} = \log P_{ri}$, $v_i = \log V_i$, $\bar{A}_0 = \bar{A}_2 = \bar{A}_4 = 1$, $\bar{A}_1 = \bar{A}_3 = 2$, $\bar{A}_5 = \bar{A}_6 = 3$, and

$$\begin{aligned} \bar{\mathbf{a}}_{01} &= [0\ 0\ 0\ 1]^T & \bar{\mathbf{a}}_{51} &= [1\ -1\ -1\ -1]^T \\ \bar{\mathbf{a}}_{11} &= [1\ 0\ 0\ 0]^T & \bar{\mathbf{a}}_{52} &= [0\ -1\ 0\ -1]^T \\ \bar{\mathbf{a}}_{12} &= [0\ 1\ 0\ 0]^T & \bar{\mathbf{a}}_{53} &= [0\ 0\ -1\ -1]^T \\ \bar{\mathbf{a}}_{21} &= [0\ 0\ 1\ 0]^T & \bar{\mathbf{a}}_{61} &= [-1\ 1\ -1\ -1]^T \\ \bar{\mathbf{a}}_{31} &= [1\ 0\ 0\ 0]^T & \bar{\mathbf{a}}_{62} &= [-1\ 0\ 0\ -1]^T \\ \bar{\mathbf{a}}_{32} &= [0\ 1\ 0\ 0]^T & \bar{\mathbf{a}}_{63} &= [0\ 0\ -1\ -1]^T \\ \bar{\mathbf{a}}_{41} &= [0\ 0\ 1\ 0]^T \end{aligned} \tag{49}$$

$$\begin{aligned} \bar{b}_{0a} &= 0 & \bar{b}_{51} &= \log\frac{N_1^{(k)}\gamma}{\Omega_2} \\ \bar{b}_{11} &= \bar{b}_{12} = \log\frac{1}{P_{T1}} & \bar{b}_{52} &= \log\frac{N_r^{(j)}\gamma}{\Omega_2} \\ \bar{b}_{21} &= \log\frac{1}{P_{T2}} & \bar{b}_{53} &= \log\frac{N_1^{(k)}\gamma}{\Omega_1} \\ \bar{b}_{31} &= \log\frac{X_3}{Q} & \bar{b}_{61} &= \log\frac{N_2^{(k)}\gamma}{\Omega_1} \\ \bar{b}_{32} &= \log\frac{X_5}{Q} & \bar{b}_{62} &= \log\frac{N_r^{(j)}\gamma}{\Omega_1} \\ \bar{b}_{41} &= \log\frac{X_4}{Q} & \bar{b}_{63} &= \log\frac{N_2^{(k)}\gamma}{\Omega_2} \end{aligned} \tag{50}$$

Because (47) and (48) are log-sum-exp functions, the optimization problem is convex. Again, the standard barrier-based interior-point method can be used to solve this GP problem. To apply this method, we must convert the inequality constrained optimization problem (47) subject to (48) into an unconstrained optimization problem. Utilizing the logarithmic barrier function, problem (47) subject to (48) is approximated as the below unconstrained optimization

problem:

$$\min_{\bar{\mathbf{p}}_i} \left\{ \bar{w}\, \bar{h}_i^{(jk)}(\bar{\mathbf{p}}_i) + \bar{\phi}_i^{(jk)}(\bar{\mathbf{p}}_i) \right\} \tag{51}$$

where $\bar{h}_i^{(jk)}(\bar{\mathbf{p}}_i)$ and $\bar{\phi}_i^{(jk)}(\bar{\mathbf{p}}_i)$ are, respectively, defined as

$$\bar{h}_i^{(jk)}(\bar{\mathbf{p}}_i) = \log \sum_{a=1}^{\bar{A}_0} \exp(\bar{\mathbf{a}}_{0a}^T \bar{\mathbf{p}}_i + \bar{b}_{0a}) \tag{52}$$

$$\bar{\phi}_i^{(jk)}(\bar{\mathbf{p}}_i) = \begin{cases} -\sum_{l=1}^{6} \log\left[-\log \sum_{a=1}^{\bar{A}_l} \exp(\bar{\mathbf{a}}_{la}^T \bar{\mathbf{p}}_i + \bar{b}_{la}) \right], & i=1 \\ -\sum_{l=1}^{3} \log\left[-\log \sum_{a=1}^{\bar{A}_l} \exp(\bar{\mathbf{a}}_{la}^T \bar{\mathbf{p}}_i + \bar{b}_{la}) \right] \\ -\sum_{l=5}^{6} \log\left[-\log \sum_{a=1}^{\bar{A}_l} \exp(\bar{\mathbf{a}}_{la}^T \bar{\mathbf{p}}_i + \bar{b}_{la}) \right], & i=2 \\ -\sum_{l=1}^{2} \log\left[-\log \sum_{a=1}^{\bar{A}_l} \exp(\bar{\mathbf{a}}_{la}^T \bar{\mathbf{p}}_i + \bar{b}_{la}) \right] \\ -\sum_{l=4}^{6} \log\left[-\log \sum_{a=1}^{\bar{A}_l} \exp(\bar{\mathbf{a}}_{la}^T \bar{\mathbf{p}}_i + \bar{b}_{la}) \right], & i=3 \\ -\sum_{l=1}^{2} \log\left[-\log \sum_{a=1}^{\bar{A}_l} \exp(\bar{\mathbf{a}}_{la}^T \bar{\mathbf{p}}_i + \bar{b}_{la}) \right] \\ -\sum_{l=5}^{6} \log\left[-\log \sum_{a=1}^{\bar{A}_l} \exp(\bar{\mathbf{a}}_{la}^T \bar{\mathbf{p}}_i + \bar{b}_{la}) \right], & i=4 \end{cases} \tag{53}$$

The barrier-method algorithm to find the solution for the optimization problem (51) is presented in Appendix B.

V. NUMERICAL RESULTS

In this section, numerical results are provided to illustrate the achievable sum-rate and outage probability of the hybrid TW-CCRN when applying the proposed optimal power allocation strategies. In particular, the sum-rate is maximized by solving the unconstrained optimization problem (34) and the outage probability is minimized by solving the unconstrained optimization problem (51). In both cases, the barrier-method algorithm given in Appendix B is used to obtain the optimal transmit powers at SU_1, SU_2, and SU_R The performance of the hybrid TW-CCRN is assessed under the effect of the following system parameters:

- Packet arrival rate λ_p at the PN
- Transmit power P_p of PU_TX
- Interference power threshold Q of PU_RX
- Maximum total transmit powers of the hybrid TW-CCRN
- Fading conditions
- Imperfect spectrum sensing

Comparisons of the performance of the hybrid TW-CCRN with and without applying the proposed power allocation strategies are also provided.

It is assumed that the hybrid TW-CCRN operates in an urban environment over Rayleigh fading channels such that channel mean powers are attenuated with distances according to the exponentially decaying path loss model with path loss exponent $n = 4$ (shadowed urban cellular radio). We denote the normalized distances of the links $\mathrm{SU}_1 \rightarrow \mathrm{SU}_\mathrm{R}$, $\mathrm{SU}_2 \rightarrow \mathrm{SU}_\mathrm{R}$, $\mathrm{SU}_1 \rightarrow \mathrm{PU}_\mathrm{RX}$, $\mathrm{SU}_\mathrm{R} \rightarrow \mathrm{PU}_\mathrm{RX}$, $\mathrm{SU}_2 \rightarrow \mathrm{PU}_\mathrm{RX}$, $\mathrm{PU}_\mathrm{TX} \rightarrow \mathrm{SU}_1$, $\mathrm{PU}_\mathrm{TX} \rightarrow \mathrm{SU}_\mathrm{R}$, and $\mathrm{PU}_\mathrm{TX} \rightarrow \mathrm{SU}_2$, respectively, as $d_1, d_2, d_3, d_4, d_5, d_6, d_7$, and d_8. In all examples, we have selected the normalized distances as

$$\begin{aligned} d_1 &= d_2 = 0.5 \\ d_3 &= d_4 = d_5 = 1.0 \\ d_6 &= d_7 = d_8 = 2.0 \end{aligned}$$

Figs. 3 and 4 depict the sum-rate and outage probability of the hybrid TW-CCRN versus arrival rate λ_p of the PN for different probabilities of imperfect spectrum sensing. Specifically, the pairs (p_f, p_m) of false alarm probability p_f and missed detection probability p_m have been chosen as $(0, 0)$, $(0.1, 0)$, $(0.2, 0)$, $(0, 0.1)$, $(0, 0.2)$, and $(0.1, 0.1)$. We fix the transmit SNR of the PN as $P_p/N_0 = 10$ dB. The maximum total transmit power-to-noise ratio of both secondary sources in the first TS and of the relay in the secondary TS are selected as $P_{T1}/N_0 = 15$ dB and $P_{T2}/N_0 = 10$ dB, respectively. In addition, we set the interference power-to-noise ratio imposed by the PN as $Q/N_0 = 5$ dB and select the departure rate of the PN as $\mu_p = 0.5$ packets/TS. Finally, the arrival and departure rates of the SN are chosen as $\lambda_s = 0.5$ packets/TS and $\mu_s = \mu_r = 0.5$ packets/TS, respectively. As can be seen from these figures, the performance of the hybrid TW-CCRN is degraded when the arrival rate of the PN increases, i.e., sum-rate decreases and outage probability increases. This is because the opportunities for the hybrid TW-CCRN to operate in interweave mode without facing the interference power constraint decreases when the amount of traffic of the PN increases. It can also be observed from Figs. 2 and 3 that the performance of the hybrid TW-CCRN is seriously reduced when the false alarm probability increases, i.e., $p_f = 0$, 0.1, and 0.2 while the missed detection probability is kept as $p_m = 0$. This is due to the fact that the SUs declare the PN as active although it is inactive which in turn reduces the time of the hybrid TW-CCRN operating in interweave mode. On the other hand, when the missed detection probability increases, i.e., $p_m = 0$, 0.1, and 0.2 while the false alarm probability is kept as $p_f = 0$, the probability that the hybrid TW-CCRN does not detect the active state of the PN and continues to operate in interweave mode increases. As a result, the performance of the hybrid TW-CCRN increases but at the expense of increased interference to the PN. For the case where both false alarm and missed detection occur, i.e., $p_f = 0.1$ and $p_m = 0.1$, the performance differs only very little from the case of perfect spectrum sensing,

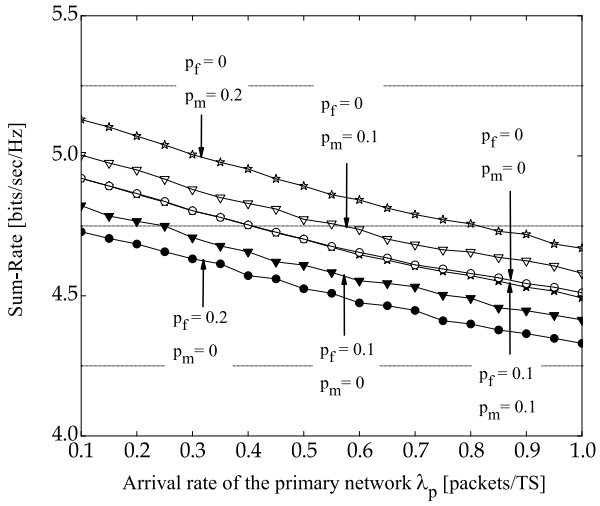

FIGURE 3. Sum-rate of the hybrid TW-CCRN versus arrival rate λ_p of the PN for different false alarm and missed detection probabilities.

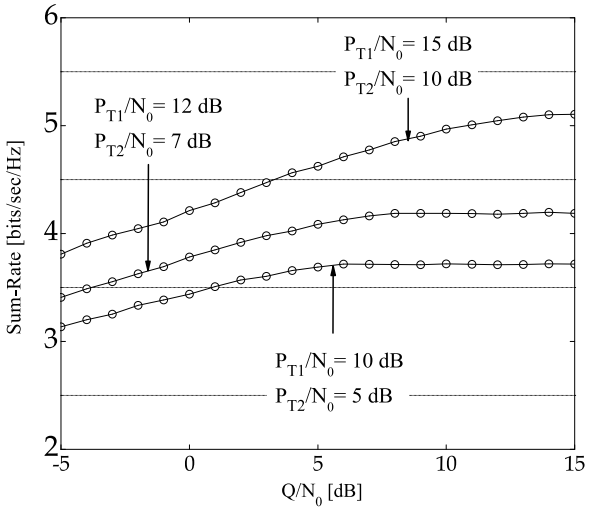

FIGURE 5. Sum-rate of the hybrid TW-CCRN versus interference power-to-noise ratio of the PN for different maximum transmit power-to-noise ratios.

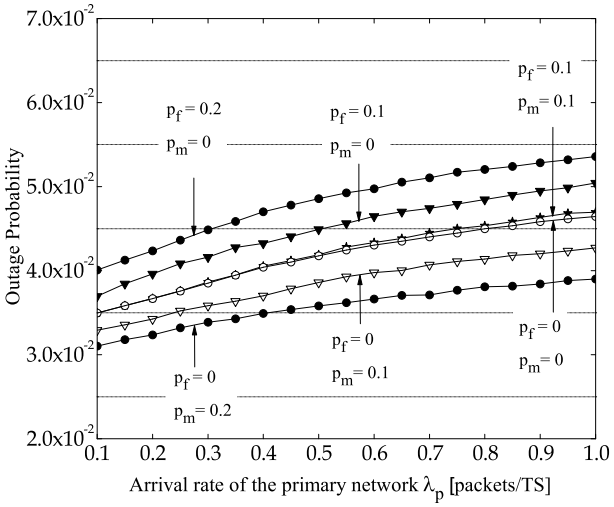

FIGURE 4. Outage probability of the hybrid TW-CCRN versus arrival rate λ_p of the PN for different false alarm and missed detection probabilities.

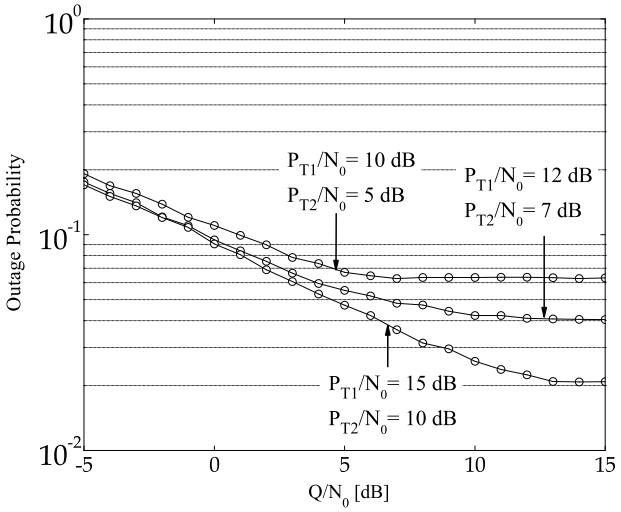

FIGURE 6. Outage probability of the hybrid TW-CCRN versus interference power-to-noise ratio of the PN for different maximum transmit power-to-noise ratios.

i.e., $p_f = 0$ and $p_m = 0$. This is because increased false alarm decreases the probability of the hybrid TW-CCRN to operate in interweave mode while increased missed detection increases the probability of the hybrid TW-CCRN to operate in interweave mode.

Figs. 5 and 6 present the sum-rate and outage probability, respectively, of the hybrid TW-CCRN versus interference power-to-noise ratio Q/N_0 of the PN for different maximum transmit power-to-noise ratios P_{T1}/N_0 and P_{T2}/N_0 in the first TS and second TS. In these examples, we select the transmit SNR of the PN as $P_p/N_0 = 5$ dB. The arrival rates and departure rates of the PN and SN are chosen as $\lambda_p = \lambda_s = 0.1$ packets/TS, and $\mu_p = \mu_s = \mu_r = 0.1$ packets/TS. As expected, when the maximum transmit power-to-noise ratios P_{T1}/N_0 and P_{T2}/N_0 increase, sum-rate and outage probability of the hybrid TW-CCRN are improved. Furthermore, if the interference power constraint of the PU becomes more relaxed, the hybrid TW-CCRN achieves better performance. Specifically, in the low Q/N_0 regime, sum-rate significantly increases and outage probability decreases as Q/N_0 increases. However, when Q/N_0 increases beyond a threshold, both the sum-rate and outage probability approach a constant floor. This behavior can be attributed to the fact that the hybrid TW-CCRN is not only affected by the interference power threshold of the PU but also by the maximum transmit power of the SUs. In particular, if the interference power-to-noise ratio becomes sufficiently high, the interference power constraint of the primary receiver becomes inactive and only the constraint on the maximum transmit power of the SUs remains active.

Figs. 7 and 8, respectively, compare the sum-rate and outage probability of the hybrid TW-CCRN with optimal power allocation and equal power allocation at SU_1, SU_2,

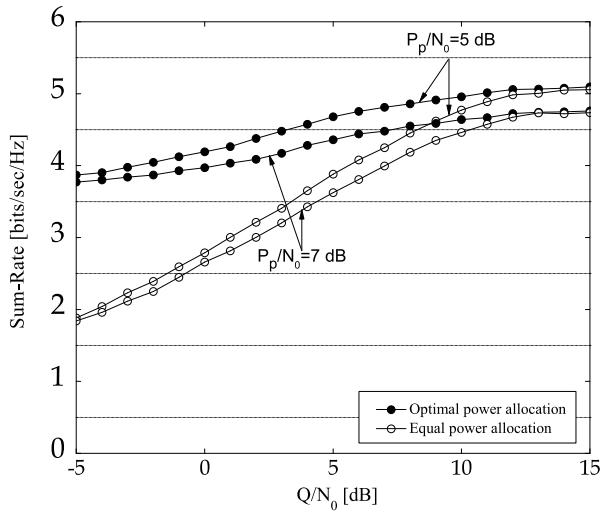

FIGURE 7. Sum-rate of the hybrid TW-CCRN with and without optimal power allocation for different transmit power-to-noise ratios P_P/N_0 of the PN.

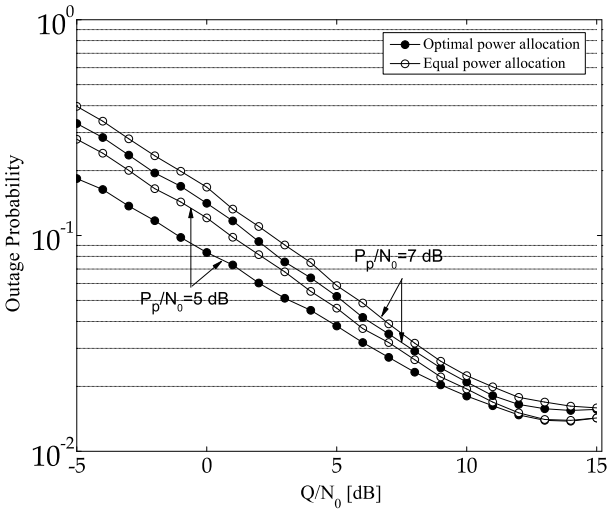

FIGURE 8. Outage probability of the hybrid TW-CCRN with and without optimal power allocation for different transmit power-to-noise ratios P_P/N_0 of the PN.

and $\mathrm{SU_R}$. For both scenarios, we select the maximum transmit power-to-noise ratio in the first and second TS as $P_{T1}/N_0 = 15$ dB and $P_{T2}/N_0 = 10$ dB, respectively. Further, the arrival and departure rates of the primary and secondary users are chosen as $\lambda_p = \lambda_s = 0.1$ packets/TS and $\mu_p = \mu_s = \mu_r = 0.5$ packets/TS, respectively. It can be clearly seen from these figures that the performance of the hybrid TW-CCRN with optimal power allocation significantly outperforms the hybrid TW-CCRN with equal power allocation in the low to medium Q/N_0 regime. Once the interference power-to-noise ratio becomes sufficiently high, both schemes converge to similar performance because the interference power constraint becomes inactive. Further, it can be observed that the performance of both schemes decreases with the increase of the transmit SNR P_p/N_0 of the PN which in turn increases the interference to the TW-CCRNs.

VI. SUMMARY

In this paper, we have proposed optimal power allocation strategies for a hybrid TW-CCRN which account for the interference power constraint of the PN as well as the transmit power limit of the hybrid TW-CCRN. In particular, optimization problems have been posed to maximize the sum-rate and to minimize the outage probability of the hybrid TW-CCRN accounting for imperfect spectrum sensing. In order to solve these problems, the decomposition method, transformation of non-convex GP into convex optimization, approximation as unconstrained optimization, and the barrier method have been applied. Our optimization framework has been carried out considering the practical issue of imperfect spectrum sensing of the hybrid TW-CCRN as well as fading conditions, and traffic characteristics of both the PN and hybrid TW-CCRN. Numerical results have been provided to illustrate the effect of system parameters such as arrival rates, interference power constraint, transmit power of the PN, false alarm and missed detection probabilities of the secondary users on the performance of the hybrid TW-CCRN. Finally, comparisons of the sum-rate and outage probability of the hybrid TW-CCRN applying the proposed optimal power allocation strategies with that of conventional equal power allocation at all terminals have been given and shown the superiority of the proposed optimal strategies.

APPENDIX A
PROBABILITY OF EACH OPERATION SCENARIO

In this appendix, we briefly describe how to calculate the probability for each operation scenario of the hybrid TW-CCRN with imperfect spectrum sensing. The interested reader is referred to [20] for a detailed derivation of the respective probabilities.

Specifically, let $p_i^{(jk)}$ denote the probability that the hybrid TW-CCRN operates in Scenario i when the PN is in State j in the first TS and in State k in the second TS. Let us recall that $j \in \{0 \triangleq$ 'inactive', $1 \triangleq$ 'active'$\}$ and $k \in \{0 \triangleq$ 'inactive', $1 \triangleq$ 'active'$\}$. Further, let us introduce the following probabilities:

- False alarm probability p_f: Probability that the SUs consider the licensed spectrum as occupied by the PU although it is inactive.
- Missed detection probability p_m: Probability that the SUs consider the licensed spectrum as vacant although it is occupied by the PU.
- Detection probability p_d: Probability that the SUs correctly sense the active state of the PU.
- No false alarm probability p_n: Probability that the SUs correctly sense the inactive state of the PU.

In addition, let p_0, p_p, p_s, p_r, p_{ps}, and p_{pr} be the steady-state probabilities that the licensed spectrum is idle, is occupied by only $\mathrm{PU_{TX}}$, by both $\mathrm{SU_1}$ and $\mathrm{SU_2}$, by only $\mathrm{SU_R}$, by $\mathrm{PU_{TX}}$, $\mathrm{SU_1}$, and $\mathrm{SU_2}$, and by both $\mathrm{PU_{TX}}$ and $\mathrm{SU_R}$, respectively. As described in [36], p_p, p_s, p_r, p_{ps}, and p_{pr} can be calculated by solving the equation $\mathbf{p} = \mathbf{A}^{-1}\mathbf{b}$ where $\mathbf{b} = [0, 0, 0, 0, 0, 1]^T$ and $\mathbf{p} = [p_0, p_p, p_s, p_r, p_{ps}, p_{pr}]^T$. Furthermore, $\mathbf{A}$ is a 6×6

matrix constructed as in (A.1), as shown at the bottom of this page, containing the arrival rate λ_p and departure rate μ_p of the PN, and the arrival rate λ_s and departure rate μ_s of the SN. Next, the probability p that the hybrid TW-CCRN is active, i.e., SU_1 and SU_2 are active in the first TS and SU_R is active in the second TS, is given by

$$p = (p_s + p_{ps})(p_r + p_{pr}) \tag{A.2}$$

According to [20], $p_i^{(jk)}$ can be computed based on the various probabilities of the imperfect spectrum sensing results and the steady-state probabilities as summarized in Table 1.

TABLE 1. Probabilities of all operation scenarios.

Scenario 1	Scenario 2
$p_1^{(11)} = \frac{p_d p_{ps} p_d p_{pr}}{(p_s+p_{ps})(p_r+p_{pr})}$	$p_2^{(11)} = \frac{p_d p_{ps} p_m p_{pr}}{(p_s+p_{ps})(p_r+p_{pr})}$
$p_1^{(10)} = \frac{p_d p_{ps} p_f p_r}{(p_s+p_{ps})(p_r+p_{pr})}$	$p_2^{(10)} = \frac{p_d p_{ps} p_n p_r}{(p_s+p_{ps})(p_r+p_{pr})}$
$p_1^{(01)} = \frac{p_f p_s p_d p_{pr}}{(p_s+p_{ps})(p_r+p_{pr})}$	$p_2^{(01)} = \frac{p_f p_s p_m p_{pr}}{(p_s+p_{ps})(p_r+p_{pr})}$
$p_1^{(00)} = \frac{p_f p_s p_f p_r}{(p_s+p_{ps})(p_r+p_{pr})}$	$p_2^{(00)} = \frac{p_f p_s p_n p_r}{(p_s+p_{ps})(p_r+p_{pr})}$
Scenario 3	**Scenario 4**
$p_3^{(11)} = \frac{p_m p_{ps} p_d p_{pr}}{(p_s+p_{ps})(p_r+p_{pr})}$	$p_4^{(11)} = \frac{p_m p_{ps} p_m p_{pr}}{(p_s+p_{ps})(p_r+p_{pr})}$
$p_3^{(10)} = \frac{p_m p_{ps} p_f p_r}{(p_s+p_{ps})(p_r+p_{pr})}$	$p_4^{(10)} = \frac{p_m p_{ps} p_n p_r}{(p_s+p_{ps})(p_r+p_{pr})}$
$p_3^{(01)} = \frac{p_n p_s p_d p_{pr}}{(p_s+p_{ps})(p_r+p_{pr})}$	$p_4^{(01)} = \frac{p_n p_s p_m p_{pr}}{(p_s+p_{ps})(p_r+p_{pr})}$
$p_3^{(00)} = \frac{p_n p_s p_f p_r}{(p_s+p_{ps})(p_r+p_{pr})}$	$p_4^{(00)} = \frac{p_n p_s p_n p_r}{(p_s+p_{ps})(p_r+p_{pr})}$

APPENDIX B
BARRIER METHOD ALGORITHM

In this section, we outline the barrier-method algorithm to find the solutions of the unconstrained optimization problems posed in (34) and (51) (see pseudo code of Algorithm 1). Let us commence with initialization of the barrier-method algorithm as follows. The initial weights on the objective functions in (34) and (51) are selected as $w_i^{(0)} = \bar{w}_i^{(0)} = 1$. The initial search points $\mathbf{p}_i^{(0)} = [p_{1i}^{(0)}, p_{2i}^{(0)}, p_{ri}^{(0)}]$ of optimization problem (34) and $\bar{\mathbf{p}}_i^{(0)} = [\bar{p}_{1i}^{(0)}, \bar{p}_{2i}^{(0)}, \bar{p}_{ri}^{(0)}, \bar{v}_i^{(0)}]$ of optimization problem (51) must be selected in the feasible region. Therefore, we choose

$$p_{1i}^{(0)} = \bar{p}_{1i}^{(0)} = \log\left[\min\left(\frac{P_{T1}}{2}, \frac{Q}{X_3}\right)\right] \tag{B.1}$$

$$p_{2i}^{(0)} = \bar{p}_{2i}^{(0)} = \log\left[\min\left(\frac{P_{T1}}{2}, \frac{Q}{X_5}\right)\right] \tag{B.2}$$

$$p_{ri}^{(0)} = \bar{p}_{ri}^{(0)} = \log\left[\min\left(\frac{P_{T2}}{2}, \frac{Q}{X_4}\right)\right] \tag{B.3}$$

We select the initial value of the auxiliary random variable as

$$\bar{v}_i^{(0)} = \log\left[\min\left(\frac{P_{T1}}{2}, \frac{Q}{X_3}, \frac{Q}{X_5}\right), \min\left(\frac{P_{T2}}{2}, \frac{Q}{X_4}\right)\right] \tag{B.4}$$

The error tolerance levels for the optimal solutions of optimization problem (34) and (51) must satisfy the following conditions: $m^{(0)}/w^{(0)} < \epsilon$ and $\bar{m}^{(0)}/\bar{w}^{(0)} < \epsilon$. Here, $m^{(0)}$ and $\bar{m}^{(0)}$ are the number of inequality constraints of (32) and (48). In our case, we select $\epsilon^{(0)} = \bar{\epsilon}^{(0)} = 10^{-3} > 0$.

Since (B.5) and (B.6) in Algorithm 1 are unconstrained convex minimization problems, they can be readily solved by a variety of iterative methods such as the gradient descent method or Newton's method. In this paper, we utilize the latter to find the optimal solution $\mathbf{p}_i^*$ and $\bar{\mathbf{p}}_i^*$.

Finally, note that the operators ∇ and ∇^2 in (B.9), (B.10), (B.11), and (B.12) used in the computation of the Newton step and decrement are defined as in [56]: 1) $\nabla f_i(\mathbf{p}_i)$ denotes the gradient vector of $f_i(\mathbf{p}_i)$, and 2) $\nabla^2 f_i(\mathbf{p}_i)$ is the Hessian matrix associated with $f_i(\mathbf{p}_i)$.

APPENDIX C
TRANSFORMATION OF A CONVEX OPTIMIZATION PROBLEM INTO AN EQUIVALENT PROBLEM USING AN AUXILIARY VARIABLE

Let us recall some findings from convex optimization related to transforming a given problem into an equivalent problem [56]. Assume that the following optimization problem is given:

$$\min_{\mathbf{x}} f_0(\mathbf{x}) \tag{C.1}$$

$$s.t. \begin{cases} f_i(\mathbf{x}) & \le 0, \quad i = 1, \ldots, m \\ h_j(\mathbf{x}) & = 0, \quad j = 1, \ldots, p \end{cases} \tag{C.2}$$

This problem is to find an optimization variable $\mathbf{x} \in \mathbb{R}^n$ that minimizes the object function $f_0(\mathbf{x})$ among all $\mathbf{x}$ such that the conditions given by the m inequality constraint functions $f_i(\mathbf{x}) \le 0,\ i = 1, \ldots, m$ and the p inequality constraint functions $h_j(\mathbf{x}) = 0,\ j = 1, \ldots, p$ are satisfied. By introducing an

$$\mathbf{A} = \begin{pmatrix} -(2\lambda_s + 2\lambda_p) & \mu_p & 0 & \mu_r & 0 & \mu_r + \mu_p \\ \lambda_p & -(2\mu_p + 2\lambda_s) & 0 & \mu_r + \lambda_p & 0 & \mu_r \\ \lambda_s & \mu_p + \lambda_s & -(2\mu_s + \lambda_p) & \mu_r + \lambda_s & 0 & \mu_p + \mu_r + \lambda_s \\ 0 & 0 & \mu_s & -(4\mu_r + 2\lambda_p + 2\lambda_s) & \mu_s + \mu_p & 0 \\ \lambda_p + \lambda_s & \lambda_s & 0 & (\mu_r + \lambda_p + \lambda_s) & -(\mu_p + 2\mu_s) & \mu_r + \lambda_s \\ 1 & 1 & 1 & 1 & 1 & 1 \end{pmatrix} \tag{A.1}$$

Algorithm 1 Barrier Method

initialize $\mathbf{p}_i \leftarrow \mathbf{p}_i^{(0)}$, $\bar{\mathbf{p}}_i \leftarrow \bar{\mathbf{p}}_i^{(0)}$, $w_i \leftarrow w_i^{(0)}$, $\bar{w}_i \leftarrow \bar{w}_i^{(0)}$, $\mu > 1$, $\epsilon^{(0)} = \bar{\epsilon}^{(0)} = 10^{-3}$

repeat

centering step Compute $\mathbf{p}_i^*$ and $\bar{\mathbf{p}}_i^*$ by minimizing the following optimization problems starting at $\mathbf{p}_i$ and $\bar{\mathbf{p}}_i$, respectively:

$$\min_{\mathbf{p}_i} f_i(\mathbf{p}_i) \tag{B.5}$$

$$\min_{\bar{\mathbf{p}}_i} \bar{f}_i(\bar{\mathbf{p}}_i) \tag{B.6}$$

where

$$f_i(\mathbf{p}_i) = w\, h_i^{(jk)}(\mathbf{p}_i) + \phi_i^{(jk)}(\mathbf{p}_i) \tag{B.7}$$

$$\bar{f}_i(\bar{\mathbf{p}}_i) = \bar{w}\, \bar{h}_i^{(jk)}(\bar{\mathbf{p}}_i) + \bar{\phi}_i^{(jk)}(\bar{\mathbf{p}}_i) \tag{B.8}$$

initialize Given starting points $\mathbf{p}_i$ and $\bar{\mathbf{p}}_i$, error tolerance $\epsilon > 0$, $\bar{\epsilon} > 0$, parameters $\alpha, \bar{\alpha} \in (0, 0.5)$, and $\beta, \bar{\beta} \in (0, 1)$.

repeat

compute Newton step and decrement

$$\mathbf{\Delta}_i = -\left(\nabla^2 f_i(\mathbf{p}_i)\right)^{-1} \nabla f_i(\mathbf{p}_i) \tag{B.9}$$

$$\lambda(\mathbf{p}_i) = \left[\nabla^T f_i(\mathbf{p}_i) \left(\nabla^2 f_i(\mathbf{p}_i)\right)^{-1} \nabla f_i(\mathbf{p}_i)\right]^{\frac{1}{2}} \tag{B.10}$$

$$\bar{\mathbf{\Delta}}_i = -\left(\nabla^2 \bar{f}_i(\bar{\mathbf{p}}_i)\right)^{-1} \nabla \bar{f}_i(\bar{\mathbf{p}}_i) \tag{B.11}$$

$$\bar{\lambda}(\bar{\mathbf{p}}_i) = \left[\nabla^T \bar{f}_i(\bar{\mathbf{p}}_i) \left(\nabla^2 \bar{f}_i(\bar{\mathbf{p}}_i)\right)^{-1} \nabla \bar{f}_i(\bar{\mathbf{p}}_i)\right]^{\frac{1}{2}} \tag{B.12}$$

line search
Compute weights w_i and $\bar{w}_i$ using the backtracking line search starting with
$w_i \leftarrow 1$, $\bar{w}_i \leftarrow 1$

while $f_i(\mathbf{p}_i + w_i \mathbf{\Delta}_i) > f_i(\mathbf{p}_i) + \alpha w_i [\nabla f_i(\mathbf{p}_i)]^T \mathbf{\Delta}_i$ **do**

$w_i \leftarrow \beta w_i$

end while

while $\bar{f}_i(\bar{\mathbf{p}}_i + \bar{w}_i \bar{\mathbf{\Delta}}_i) > \bar{f}_i(\bar{\mathbf{p}}_i) + \bar{\alpha} \bar{w}_i [\nabla \bar{f}_i(\bar{\mathbf{p}}_i)]^T \bar{\mathbf{\Delta}}_i$ **do**

$\bar{w}_i \leftarrow \bar{\beta} \bar{w}_i$

end while

update $\mathbf{p}_i \leftarrow \mathbf{p}_i + w_i \mathbf{\Delta}_i$ and $\bar{\mathbf{p}}_i \leftarrow \bar{\mathbf{p}}_i + \bar{w}_i \bar{\mathbf{\Delta}}_i$.

until $\lambda^2(\mathbf{p}_i)/2 \leq \epsilon$ and $\bar{\lambda}^2(\bar{\mathbf{p}}_i)/2 \leq \bar{\epsilon}$

update $\mathbf{p}_i^* \leftarrow \mathbf{p}_i$, $\bar{\mathbf{p}}_i^* \leftarrow \bar{\mathbf{p}}_i$, $w_i \leftarrow \mu_i w_i$, $\bar{w}_i \leftarrow \bar{\mu}_i \bar{w}_i$

until $m_i/w_i < \epsilon$ and $\bar{m}_i/\bar{w}_i < \bar{\epsilon}$

auxiliary variable $t \geq f_0(\mathbf{x})$, the standard optimization problem (C.1) subject to (C.2) can be transformed into equivalent Epigraph problem form [56] given as

$$\min_{\mathbf{x},t} t \tag{C.3}$$

$$s.t. \begin{cases} f_0(\mathbf{x}) \leq t \\ f_i(\mathbf{x}) \leq 0, \quad i = 1, \ldots, m \\ h_j(\mathbf{x}) = 0 \quad j = 1, \ldots, p \end{cases} \tag{C.4}$$

In our case, in the context of minimizing the outage probability of the hybrid TW-CCRN, we consider the following optimization problem:

$$\min_{P_{1i}P_{2i},P_{ri}} \max\left\{F_{\gamma_{1i}^{(jk)}}(\gamma_{th1}), F_{\gamma_{2i}^{(jk)}}(\gamma_{th2})\right\} \tag{C.5}$$

$$s.t. \begin{cases} P_{1i}, P_{2i}, P_{ri} & > 0 \\ P_{1i} + P_{2i} & \leq P_{T1} \\ P_{ri} & \leq P_{T2} \\ 1_{[i=1 \text{ or } 2]}(P_{1i}X_3 + P_{2i}X_5) & \leq Q \\ 1_{[i=1 \text{ or } 3]}P_{ri}X_4 & \leq Q \end{cases} \tag{C.6}$$

By introducing the positive auxiliary variable $V_i = \max\left\{F_{\gamma_{1i}^{(jk)}}(\gamma_{th1}), F_{\gamma_{2i}^{(jk)}}(\gamma_{th2})\right\}$, the standard optimization problem (C.5) subject to (C.6) can be transformed into the following equivalent Epigraph problem form:

$$\min_{P_{1i}P_{2i},P_{ri},V_i} V_i \tag{C.7}$$

$$s.t. \begin{cases} P_{1i}, P_{2i}, P_{ri}, V_i & > 0 \\ P_{1i} + P_{2i} & \leq P_{T1} \\ P_{ri} & \leq P_{T2} \\ 1_{[i=1 \text{ or } 2]}(P_{1i}X_3 + P_{2i}X_5) & \leq Q \\ 1_{[i=1 \text{ or } 3]}P_{ri}X_4 & \leq Q \\ \max\left\{F_{\gamma_{1i}^{(jk)}}(\gamma_{th1}), F_{\gamma_{2i}^{(jk)}}(\gamma_{th2})\right\} & \leq V_i \end{cases} \tag{C.8}$$

Then, it is straightforward to obtain the following equivalent optimization problem:

$$\min_{P_{1i}P_{2i},P_{ri},V_i} V_i \tag{C.9}$$

$$s.t. \begin{cases} P_{1i}, P_{2i}, P_{ri}, V_i & > 0 \\ P_{1i} + P_{2i} & \leq P_{T1} \\ P_{ri} & \leq P_{T2} \\ 1_{[i=1 \text{ or } 2]}(P_{1i}X_3 + P_{2i}X_5) & \leq Q \\ 1_{[i=1 \text{ or } 3]}P_{ri}X_4 & \leq Q \\ F_{\gamma_{1i}^{(jk)}}(\gamma_{th1}) & \leq V_i \\ F_{\gamma_{2i}^{(jk)}}(\gamma_{th2}) & \leq V_i \end{cases} \tag{C.10}$$

REFERENCES

[1] *Spectrum Policy Task Force Report*, document ET Docket 02-135, Federal Communications Commission, Nov. 2002.

[2] *Cognitive Radio Technology—A study for Ofcom*, document QINETIQ/06/00420, nr. 1.1, QinetuQ, Feb. 2007.

[3] V. Valenta and R. Maršálek, G. Baudoin, M. Villegas, M. Suarez, and F. Robert, "Survey on spectrum utilization in Europe: Measurements, analyses and observations," in *Proc. Int. ICST Conf. Cognit. Radio Oriented Wireless Netw. Commun.*, Cannes, France, Jun. 2010, pp. 1–5.

[4] J. Mitola and G. Q. Maguire, Jr., "Cognitive radio: Making software radios more personal," *IEEE Pers. Commun.*, vol. 6, no. 4, pp. 13–18, Apr. 1999.

[5] A. Goldsmith, S. A. Jafar, and I. Marić, and S. Srinivasa, "Breaking spectrum gridlock with cognitive radios: An information theoretic perspective," *Proc. IEEE*, vol. 97, no. 5, pp. 894–914, May 2009.

[6] Y. Xing, R. Chandramouli, S. Mangold, and N. Sai Shankar, "Dynamic spectrum access in open spectrum wireless networks," *IEEE J. Sel. Areas Commun.*, vol. 24, no. 3, pp. 626–637, Mar. 2006.

[7] X. Kang, Y.-C. Liang, and A. Nallanathan, "Optimal power allocation for fading channels in cognitive radio networks under transmit and interference power constraints," in *Proc. IEEE Int. Conf. Commun.*, Beijing, China, May 2008, pp. 3568–3572.

[8] V. A. Bohara, S. H. Ting, Y. Han, and A. Pandharipande, "Interference-free overlay cognitive radio network based on cooperative space time coding," in *Proc. Cognit. Radio Oriented Wireless Netw. Commun.*, Cannes, France, Jun. 2010, pp. 1–5.

[9] Q. Zhang, J. Jia, and J. Zhang, "Cooperative relay to improve diversity in cognitive radio networks," *IEEE Commun. Mag.*, vol. 47, no. 2, pp. 111–117, Feb. 2009.

[10] T. M. C. Chu, T. Q. Duong, and H.-J. Zepernick, "MRT/MRC for cognitive AF relay networks under feedback delay and channel estimation error," in *Proc. IEEE Int. Symp. Pers., Indoor Mobile Radio Commun.*, Sydney, NSW, Australia, Sep. 2012, pp. 2184–2189.

[11] T. M. C. Chu, H. Phan, T. Q. Duong, M. Elkashlan, and H.-J. Zepernick, "Beamforming transmission in cognitive AF relay networks with feedback delay," in *Proc. IEEE Int. Conf. Comput., Manage. Telecommun.*, Ho Chi Minh City, Vietnam, Jan. 2013, pp. 117–122.

[12] T. M. C. Chu, H. Phan, and H.-J. Zepernick, "MIMO incremental AF relay networks with TAS/MRC and adaptive modulation," in *Proc. IEEE Veh. Technol. Conf.*, Las Vegas, NV, USA, Sep. 2013, pp. 1–5.

[13] T. M. C. Chu, H. Phan, and H.-J. Zepernick, "Adaptive modulation and coding with queue awareness in cognitive incremental decode-and-forward relay networks," in *Proc. IEEE Int. Conf. Commun.*, Sydney, NSW, Australia, Jun. 2014, pp. 1453–1459.

[14] T. M. C. Chu, H. Phan, and H.-J. Zepernick, "Performance analysis of MIMO cognitive amplify-and-forward relay networks with orthogonal space-time block codes," *Wireless Commun. Mobile Comput.*, vol. 15, no. 12, pp. 1659–1679, Jan. 2015.

[15] L. Li, X. Zhou, H. Xu, G. Y. Li, D. Wang, and A. Soong, "Simplified relay selection and power allocation in cooperative cognitive radio systems," *IEEE Trans. Wireless Commun.*, vol. 10, no. 1, pp. 33–36, Jan. 2011.

[16] G. Zhao, C. Yang, G. Y. Li, D. Li, and A. C. K. Soong, "Power and channel allocation for cooperative relay in cognitive radio networks," *IEEE J. Sel. Topics Signal Process.*, vol. 5, no. 1, pp. 151–159, Feb. 2011.

[17] H. Yu, W. Tang, and S. Li, "Joint optimal sensing time and power allocation for amplify-and-forward cognitive relay networks," *IEEE Commun. Lett.*, vol. 16, no. 12, pp. 1948–1951, Dec. 2012.

[18] M. Naeem, K. Illanko, A. K. Karmokar, A. Anpalagan, and M. Jaseemuddin, "Power allocation in decode and forward relaying for green cooperative cognitive radio systems," in *Proc. IEEE Wireless Commun. Netw. Conf.*, Shanghai, China, Apr. 2013, pp. 3806–3810.

[19] N. Mokari, S. Parsaeefard, H. Saeedi, and P. Azmi, "Cooperative secure resource allocation in cognitive radio networks with guaranteed secrecy rate for primary users," *IEEE Trans. Wireless Commun.*, vol. 13, no. 2, pp. 1058–1073, Feb. 2014.

[20] T. M. C. Chu and H.-J. Zepernick, "Optimal power allocation for hybrid cognitive cooperative radio networks with imperfect spectrum sensing," *IEEE Access*, vol. 6, pp. 10365–10380, 2018.

[21] K. Jitvanichphaibool, Y.-C. Liang, and R. Zhang, "Beamforming and power control for multi-antenna cognitive two-way relaying," in *Proc. IEEE Wireless Commun. Netw. Conf.*, Budapest, Hungary, Apr. 2009, pp. 1–6.

[22] P. Ubaidulla and S. Aïssa, "Optimal relay selection and power allocation for cognitive two-way relaying networks," *IEEE Wireless Commun. Lett.*, vol. 1, no. 3, pp. 225–228, Jun. 2012.

[23] A. Alsharoa, F. Bader, and M.-S. Alouini, "Relay selection and resource allocation for two-way DF-AF cognitive radio networks," *IEEE Wireless Commun. Lett.*, vol. 2, no. 4, pp. 427–430, Aug. 2013.

[24] A. Alsharoa, H. Ghazzai, and M.-S. Alouini, "Optimal transmit power allocation for MIMO two-way cognitive relay networks with multiple relays using AF strategy," *IEEE Wireless Commun. Lett.*, vol. 3, no. 1, pp. 30–33, Feb. 2014.

[25] A. Alsharoa, H. Ghazzai, E. Yaacoub, M.-S. Alouini, and A. E. Kamal, "Joint bandwidth and power allocation for MIMO two-way relays-assisted overlay cognitive radio systems," *IEEE Trans. Cogn. Commun. Netw.*, vol. 1, no. 4, pp. 383–393, Dec. 2015.

[26] L. Sboui, H. Ghazzai, Z. Rezki, and M.-S. Alouini, "On achievable rate of two-way relaying cognitive radio with space alignment," in *Proc. IEEE Int. Conf. Commun.*, London, U.K., Jun. 2015, pp. 7628–7632.

[27] A. Z. Ghanavati and D. C. Lee, "Max-min optimization of transmission powers in the two-way cognitive radio network assisted by orthogonally signaling relays," in *Proc. IEEE Annu. Inf. Technol., Electron. Mobile Commun. Conf.*, Vancouver, BC, Canada, Nov. 2017, pp. 458–463.

[28] S. Vahidian, M. Najafi, M. Najafi, and F. S. Al-Qahtani, "Power allocation and cooperative diversity in two-way non-regenerative cognitive radio networks," in *Proc. IEEE Int. Conf. Commun.*, Paris, France, May 2017, pp. 1–7.

[29] S. Mittal, N. Gupta, V. A. Bohara, D. B. da Costa, and U. S. Dias, "A cooperative spectrum sharing protocol for cognitive two-way AF relaying system," in *Proc. IEEE Region 10 Symp.*, Cochin, India, Jul 2017, pp. 1–5.

[30] V. Chakravarthy *et al.*, "Novel overlay/underlay cognitive radio waveforms using SD-SMSE framework to enhance spectrum efficiency—Part I: Theoretical framework and analysis in AWGN channel," *IEEE Trans. Commun.*, vol. 57, no. 12, pp. 3794–3804, Dec. 2009.

[31] V. Chakravarthy, X. Li, R. Zhou, Z. Wu, and M. Temple, "Novel overlay/underlay cognitive radio waveforms using SD-SMSE framework to enhance spectrum efficiency—Part II: Analysis in fading channels," *IEEE Trans. Commun.*, vol. 58, no. 6, pp. 1868–1876, Jun. 2010.

[32] M. C. Filippou, G. A. Ropokis, D. Gesbert, and T. Ratnarajah, "Joint sensing and reception design of SIMO hybrid cognitive radio systems," *IEEE Trans. Wireless Commun.*, vol. 15, no. 9, pp. 6327–6341, Sep. 2016.

[33] A. Kaushik, S. K. Sharma, S. Chatzinotas, B. Ottersten, and F. Jondral, "Performance analysis of hybrid cognitive radio systems with imperfect channel knowledge," in *Proc. IEEE Int. Conf. Commun.*, Kuala Lumpur, Malaysia, May 2016, pp. 1–7.

[34] D. Wang, N. Zhang, Z. Li, F. Gao, and X. Shen, "Leveraging high order cumulants for spectrum sensing and power recognition in cognitive radio networks," *IEEE Trans. Wireless Commun.*, vol. 17, no. 2, pp. 1298–1310, Feb. 2018.

[35] J. B. Si, Z. Li, J. J. Chen, and H. Y. Huang, "On the performance of cognitive relay networks with cooperative spectrum sensing," in *Proc. IEEE Int. Conf. Commun.*, Ottawa, ON, Canada, Jun. 2012, pp. 1709–1714.

[36] T. M. C. Chu, H. Phan, and H.-J. Zepernick, "Hybrid interweave-underlay spectrum access for cognitive cooperative radio networks," *IEEE Trans. Commun.*, vol. 62, no. 7, pp. 2183–2197, Jul. 2014.

[37] H. Yazdani and A. Vosoughi, "On cognitive radio systems with directional antennas and imperfect spectrum sensing," in *Proc. IEEE Int. Conf. Acoust., Speech Signal Process.*, New Orleans, LA, USA, Mar. 2017, pp. 3589–3593.

[38] A. U. Rehman, L.-L. Yang, and L. Hanzo, "Delay and throughput analysis of cognitive go-back-N HARQ in the face of imperfect sensing," *IEEE Access*, vol. 5, pp. 7454–7473, 2017.

[39] A. U. Rehman, C. Dong, L.-L. Yang, and L. Hanzo, "Performance of cognitive stop-and-wait hybrid automatic repeat request in the face of imperfect sensing," *IEEE Access*, vol. 4, pp. 5489–5508, Sep. 2016.

[40] H. Zhang, Y. Nie, J. Cheng, V. C. M. Leung, and A. Nallanathan, "Sensing time optimization and power control for energy efficient cognitive small cell with imperfect hybrid spectrum sensing," *IEEE Trans. Wireless Commun.*, vol. 16, no. 2, pp. 730–743, Feb. 2017.

[41] G. Ozcan, M. C. Gursoy, N. Tran, and J. Tang, "Energy-efficient power allocation in cognitive radio systems with imperfect spectrum sensing," *IEEE J. Sel. Areas Commun.*, vol. 34, no. 12, pp. 3466–3481, Dec. 2016.

[42] L. Zhu and X. Zhao, "Robust power allocation for orthogonal frequency division multiplexing-based overlay/underlay cognitive radio network under spectrum sensing errors and channel uncertainties," *IET Commun.*, vol. 10, no. 15, pp. 2010–2017, Oct. 2016.

[43] F. Zhou, N. C. Beaulieu, J. Cheng, Z. Chu, and Y. Wang, "Robust max–min fairness resource allocation in sensing-based wideband cognitive radio with SWIPT: Imperfect channel sensing," *IEEE Syst. J.*, vol. 12, no. 3, pp. 2361–2372, Sep. 2018.

[44] X. Kang, Y. C. Liang, H. K. Garg, and L. Zhang, "Sensing-based spectrum sharing in cognitive radio networks," *IEEE Trans. Veh. Technol.*, vol. 58, no. 8, pp. 4649–4654, Oct. 2009.

[45] X. Zhang and H. Su, "CREAM-MAC: Cognitive radio-enabled multi-channel MAC protocol over dynamic spectrum access networks," *IEEE J. Sel. Areas Commun.*, vol. 5, no. 1, pp. 110–123, Feb. 2011.

[46] Y.-C. Liang, Y. Zeng, E. C. Y. Peh, and A. T. Hoang, "Sensing-throughput tradeoff for cognitive radio networks," *IEEE Trans. Wireless Commun.*, vol. 7, no. 4, pp. 1326–1337, Apr. 2008.

[47] M. Aljuaid and H. Yanikomeroglu, "Investigating the Gaussian convergence of the distribution of the aggregate interference power in large wireless networks," *IEEE Trans. Veh. Technol.*, vol. 59, no. 9, pp. 4418–4424, Nov. 2010.

[48] H. Inaltekin, "Gaussian approximation for the wireless multi-access interference distribution," *IEEE Trans. Signal Process.*, vol. 60, no. 11, pp. 6114–6120, Nov. 2012.
[49] C.-S. Yeh and Y. Lin, "Channel estimation using pilot tones in OFDM systems," *IEEE Trans. Broadcast.*, vol. 45, no. 4, pp. 400–409, Dec. 1999.
[50] R. Kudo, J. McGeehan, S. M. D. Armour, and M. Mizoguchi, "CSI estimation method based on random beamforming for massive number of transmit antenna systems," in *Proc. IEEE Int. Symp. Wireless Commun. Syst.*, Paris, France, Aug. 2012, pp. 716–720.
[51] R. Kudo, S. M. D. Armour, J. P. McGeehan, and M. Mizoguchi, "A channel state information feedback method for massive MIMO-OFDM," *J. Commun. Netw.*, vol. 15, no. 4, pp. 352–361, Aug. 2013.
[52] Z. Shu, J. Zhou, Y. Yang, H. Sharif, and Y. Qian, "Network coding-aware channel allocation and routing in cognitive radio networks," in *Proc. IEEE Global Commun. Conf.*, Anaheim, CA, USA, Dec. 2012, pp. 5590–5595.
[53] R. Zhang, S. Cui, and Y.-C. Liang, "On ergodic sum capacity of fading cognitive multiple-access and broadcast channels," *IEEE Trans. Inf. Theory*, vol. 55, no. 11, pp. 5161–5178, Nov. 2009.
[54] M. Chiang, "Geometric programming for communication systems," *Found. Trends Commun. Inf. Theory*, vol. 2, nos. 1–2, pp. 1–154, Aug. 2005.
[55] S. Boyd, S.-J. Kim, L. Vandenberghe, and A. Hassibi, "A tutorial on geometric programming," *Optim. Eng.*, vol. 8, no. 1, pp. 67–127, 2007.
[56] S. Boyd and L. Vandenberghe, *Convex Optimization*. Cambridge, U.K.: Cambridge Univ. Press, 2004.
[57] X. Kang, R. Zhang, Y.-C. Liang, and H. K. Garg, "Optimal power allocation strategies for fading cognitive radio channels with primary user outage constraint," *IEEE J. Sel. Areas Commun.*, vol. 29, no. 2, pp. 374–383, Feb. 2011.
[58] I. S. Gradshteyn and I. M. Ryzhik, *Table of Integrals, Series, and Products*, 7th ed. New York, NY, USA: Academic, 2007.
[59] Y. Li, X. Zhang, M. Peng, and W. Wang, "Power provisioning and relay positioning for two-way relay channel with analog network coding," *IEEE Signal Process. Lett.*, vol. 18, no. 9, pp. 517–520, Sep. 2011.

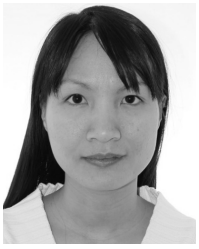

THI MY CHINH CHU (M'17) received the B.S. and M.Sc. degrees in electronics and communications from the Hanoi University of Science and Technology, Vietnam, in 2004 and 2007, respectively, and the Ph.D. degree in telecommunication systems with the Radio Communications Group, Blekinge Institute of Technology, Sweden, in 2015. From 2004 to 2010, she was with the Radio Broadcasting of Vietnam, the Voice of Vietnam. She is currently a Research Fellow at the Blekinge Institute of Technology. Her current research interests include cooperative communications, cognitive radio networks, mobile multimedia, quality of experience, and perceptual quality assessment.

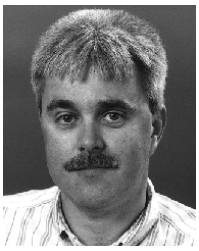

HANS-JÜRGEN ZEPERNICK (M'94–SM'11) received the Dipl.-Ing. degree from the University of Siegen, Germany, in 1987, and the Dr.-Ing. degree from the University of Hagen, Germany, in 1994. From 1987 to 1989, he was with Siemens AG, Germany. He was a Professor of wireless communications at Curtin University of Technology, a Deputy Director of the Australian Telecommunications Research Institute, and an Associate Director of the Australian Telecommunications Cooperative Research Centre. He is currently a Professor of radio communications at the Blekinge Institute of Technology, Sweden. His research interests include cooperative communications, cognitive radio networks, immersive mobile multimedia, and perceptual quality assessment. He has been serving as a Technical Program Committee Member for several international conferences, such as IEEE GLOBECOM, IEEE ICC, IEEE PIMRC, IEEE VTC, and IEEE WCNC. He has served as the Chair of the track Cognitive Radio and Spectrum Management of IEEE VTC-Spring 2016.